(12) INTERNATIONAL APPLICATION PUBLISHED UNDER THE PATENT COOPERATION TREATY (PCT)

(19) World Intellectual Property Organization
International Bureau

(43) International Publication Date
8 July 2010 (08.07.2010)

PCT

(10) International Publication Number
WO 2010/077819 A1

(51) International Patent Classification:
H04B 1/10 (2006.01)

(21) International Application Number:
PCT/US2009/067886

(22) International Filing Date:
14 December 2009 (14.12.2009)

(25) Filing Language: English

(26) Publication Language: English

(30) Priority Data:
12/346,146 30 December 2008 (30.12.2008) US

(71) Applicant *(for all designated States except US)*: **TRUEPOSITION INC.** [US/US]; 1000 Chesterbrook Boulevard, Berwyn, PA 19312 (US).

(72) Inventors; and

(75) Inventors/Applicants *(for US only)*: **BOYER, Pete, A.** [US/US]; 52 Rampart Drive, Chesterbrook, PA 19087 (US). **MIA, Rashidus, S.** [US/US]; 113 Peter Dehaven Drive, Phoenixville, PA 19460 (US). **SEGALL, Edward, Joseph** [US/US]; 235 Lona Avenue, Narberth, PA 19072 (US).

(74) Agent: **STEIN, Michael, D.**; Woodcock Washburn LLP, Cira Centre, 12th Floor, 2929 Arch Street, Philadelphia, PA 19104-2891 (US).

(81) Designated States *(unless otherwise indicated, for every kind of national protection available)*: AE, AG, AL, AM, AO, AT, AU, AZ, BA, BB, BG, BH, BR, BW, BY, BZ, CA, CH, CL, CN, CO, CR, CU, CZ, DE, DK, DM, DO, DZ, EC, EE, EG, ES, FI, GB, GD, GE, GH, GM, GT, HN, HR, HU, ID, IL, IN, IS, JP, KE, KG, KM, KN, KP, KR, KZ, LA, LC, LK, LR, LS, LT, LU, LY, MA, MD, ME, MG, MK, MN, MW, MX, MY, MZ, NA, NG, NI, NO, NZ, OM, PE, PG, PH, PL, PT, RO, RS, RU, SC, SD, SE, SG, SK, SL, SM, ST, SV, SY, TJ, TM, TN, TR, TT, TZ, UA, UG, US, UZ, VC, VN, ZA, ZM, ZW.

(84) Designated States *(unless otherwise indicated, for every kind of regional protection available)*: ARIPO (BW, GH, GM, KE, LS, MW, MZ, NA, SD, SL, SZ, TZ, UG, ZM, ZW), Eurasian (AM, AZ, BY, KG, KZ, MD, RU, TJ, TM), European (AT, BE, BG, CH, CY, CZ, DE, DK, EE, ES, FI, FR, GB, GR, HR, HU, IE, IS, IT, LT, LU, LV, MC, MK, MT, NL, NO, PL, PT, RO, SE, SI, SK, SM, TR), OAPI (BF, BJ, CF, CG, CI, CM, GA, GN, GQ, GW, ML, MR, NE, SN, TD, TG).

[Continued on next page]

(54) Title: METHOD FOR POSITION ESTIMATION USING GENERALIZED ERROR DISTRIBUTIONS

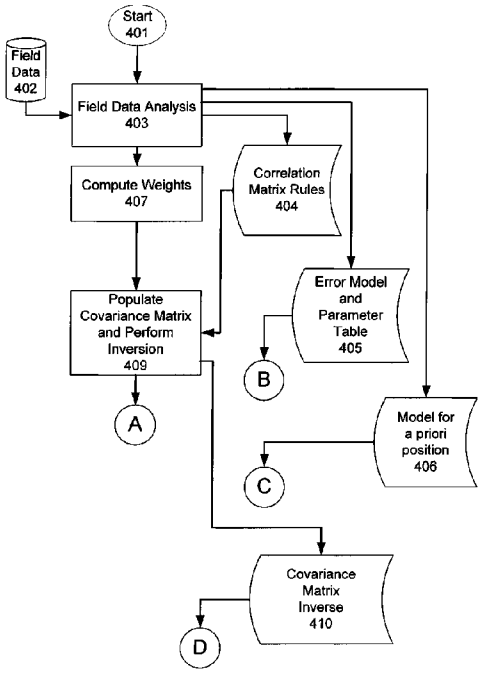

Figure 4a

(57) Abstract: A method for improving the results of radio location systems that incorporate weighted least squares optimization generalizes the weighted least squares method by using maximum a posteriori (MAP) probability metrics to incorporate characteristics of the specific positioning problem (e.g., UTDOA). Weighted least squares methods are typically used by TDOA and related location systems including TDOA/AOA and TDOA/GPS hybrid systems. The incorporated characteristics include empirical information about TDOA errors and the probability distribution of the mobile position relative to other network elements. A technique is provided for modeling the TDOA error distribution and the a priori mobile position. A method for computing a MAP decision metric is provided using the new probability distribution models. Testing with field data shows that this method yields significant improvement over existing weighted least squares methods.

WO 2010/077819 A1

Published:

— *with international search report (Art. 21(3))*

METHOD FOR POSITION ESTIMATION USING GENERALIZED ERROR DISTRIBUTIONS

CROSS REFERENCE TO RELATED APPLICATIONS

[0001] This application claims priority to U.S. Patent Application Number 12/346,146 filed December 30, 2008, which is incorporated herein by reference in its entirety.

TECHNICAL FIELD

[0002] The present application relates generally to the field of wireless location, i.e., systems and methods for estimating the position of a wireless device, and more particularly to a method using generalized error distributions.

BACKGROUND

[0003] As the Federal Communications Commission (FCC) moves towards a PSAP-level location accuracy mandate, improving methods for different location technologies becomes a necessity. The subject matter described herein relates to the fields of communications and location technology. It provides a means for improving the accuracy of location technologies such as Global Positioning System (GPS), Uplink Time Difference of Arrival (UTDOA) and Advanced Forward Link Trilateration (AFLT).

[0004] A common approach to position estimation is to find a *weighted least squares* solution from measured quantities such as time differences, pseudoranges or power levels. The weighted least squares solution is known to achieve a maximum likelihood (ML) solution when input errors are independent and Gaussian (see J. Caffery, *Wireless Location in CDMA Cellular Radio Systems*, Boston-London: Kluwer Academic Publishers, 2000), but it cannot do this under the more general conditions encountered in practice. For example, TDOA errors have a tendency to be positive relative to the predicted leading edge of the multipath delay profile. As explained below, several factors such as imperfect leading edge detection and non-line-of-sight (NLOS) propagation contribute to these positive errors. As a result, the per-baseline error distribution is skewed. This skew reduces the accuracy of the basic weighted least squares method. In contrast, the method described herein exploits knowledge of this skew to obtain improved results. Moreover, correlation among these errors can often be found; for example, distinct multipath components can be received at the same

sector, common NLOS conditions may exist at a site and common errors may be introduced by the reference signal. These correlations may be incorporated into a *maximum a posteriori* (MAP) algorithm as described below. This framework can also be used to incorporate an estimate of the *a priori* mobile position distribution in the location solution.

[0005] UTDOA is a network-based technology allowing for any signal transmitted from any type of mobile station (MS) to be received at any base station to obtain a UTDOA measurement. A reference base station measures the received signal at roughly the same time as each cooperating base station, as illustrated in Figure 1.

[0006] Figure 1 shows an idealized model of the signals available to or from a mobile device for positioning where the present invention could be used to increase the accuracy of the positioning estimate (also called a location attempt). This figure also identifies the system components for wireless location. In Figure 1, a Global Navigation Satellite System 101 (GNSS) such as the United States NavStar Global Positioning System (GPS), broadcasts well defined, code division multiple access (CDMA) spread spectrum signals 107 used by specially equipped mobile wireless devices 102 for TDOA location estimation of latitude, longitude, altitude and velocity. If the mobile device 102 is not equipped to receive satellite signals 107 for location calculation, both uplink and downlink terrestrial wireless techniques using TDOA or Time-of-Arrival (TOA) calculations may be used to provide a location estimate. Terrestrial wide area wireless location techniques using downlink (network based transmitter-to-device) TDOA or TOA techniques include Advanced Forward Link Trilateration (FLT) [IS-95, IS-2000], Enhanced Time Difference of Arrival (E-OTD) [GSM] and Observed Time Difference of Arrival (OTDOA) [UMTS] as well as distributed beacon techniques. Terrestrial Downlink techniques require that the mobile device 102 measure the downlink radio signals 108 from network based transmitters 103 104 and then use the radio link(s) 109, backhaul facilities 113 and the Wireless Communications Network 110 to convey the collected radio measurements to a Position Determining Entity (PDE) 106 for conversion into a latitude, longitude and in some cases an altitude.

[0007] Terrestrial wide area wireless location techniques using uplink (device-to-network based receiver) TDOA or TOA techniques include U-TDOA, U-TDOA/Angle of Arrival (AoA) hybrid and U-TDOA/Assisted GPS. U-TDOA and hybrids currently function in CDMA [IS-95, IS-2000], GSM, UMTS, WiMAX (802.16e/m and 802.20) and conceptually for the upcoming Long-Term-Evolution (LTE) OFDM based wireless radio access network (RAN). Terrestrial Uplink techniques require that the mobile device 102 transmissions 109 be measured by network based receivers (in this case co-located within the

cell sites 103 104. Measurement data is then conveyed by backhaul 111 to a Position Determining Entity (PDE) 106 for conversion into a latitude, longitude, velocity, and in some cases an altitude. Regardless of the aforementioned wireless location technique, determination of the radio signal time-of-flight is key to accurate determination of the mobile devices 102 actual location. In Figure 1, the real world influences of signal reflection, diffraction, and attenuation due to constructive or destructive interference are not shown.

[0008] In the system of Figure 1, by cross-correlating the received signal at the reference base station with the received signal at a cooperating base station, a time difference of arrival is determined. The cooperating stations send their TDOA measurements to a position determining entity (PDE) where a location solution is found. However, impairments to the measurement can arise from additive noise and signal level fluctuations. These impairments may affect the sensitivity of detecting the presence of the mobile signal at the cooperating base station. Other impairments to the estimation impact the cooperator's ability to detect the line of sight (LOS) path delay.

[0009] Figures 2a, 2b, 2c and 2d illustrate how objects, such as a building, may block the direct path, creating a non-line of sight impairment in different location environments, including uplink, downlink, GNSS and hybrid GNSS/uplink systems (where GNSS stands for Global Navigation Satellite System). A diffracted path traveling around a building arrives at the receiver later than the highly attenuated or completely blocked direct path. Additionally, reflections from obstacles can cause scattering, which produces dispersion of the arrival times of different paths. In Figure 2a, an example of an uplink wireless location system is depicted. The mobile device 102 transmits a signal 109. In some cases, such as for the Reference Receiver 203, the radio signal is received directly (a line-of-sight or LOS case). But other receivers 104 may receive diffracted signal 202 or a reflected signal 203. In each case the original uplink signal 109 may also be received or have the original signal blocked, attenuated or delayed by an obstruction 201.

[0010] Figure 3 illustrates impairments that make detection of the first arrival difficult and cause a skewing of the TDOA error. The reference numerals in Figure 3 are used as follows:

303 = Transmit time

304 = Detection threshold

305 = Line-of-sight (LOS) time-of-flight

306 = Lag time

307 = Basis for reported TOA or TDOA

308 = Delay spread

309 = Missed signal components

[0011] Figure 3 shows the arrival times of a multi-path degraded signal on an amplitude 302 to time 301 plot 300. A signal is transmitted at time 303 and has a potential direct path time-of-flight shown as 305. The earliest signal component arrivals are undetected since they arrive at a power level below the detection threshold 304. The detection threshold 304 must be maintained to avoid excessive false alarms. Missed earliest arrival detection events cause a reported TOA or TDOA that is larger than the LOS TOA or TDOA which is desired. In this example the first signal above threshold 307 produces a lag of 306 from the true first arriving signal component. Additionally, the earliest arriving multipath components may arrive later than expected due to NLOS propagation creating an NLOS delay. This also causes a reported TDOA that is larger than the LOS TDOA. These factors skew errors between the TDOA measurements and an LOS TDOA being searched or computed by positioning algorithms. Positioning decisions in the inventive solution described herein exploit both the skewing of errors caused by these factors as well as the non-Gaussian shape of the error distribution.

[0012] The method described in U. S. Patent 6,564,065, May 13, 2003, K. Chang et al., "Bayesian-update based location prediction method for CDMA Systems," appears to predict power levels from CDMA pilot channel measurements with location decisions made from an *a posteriori* power distribution using simulation. The method described in U. S. Patent 5,252,982, Oct. 12, 1993, E. Frei, "Method of precise position determination," appears to assume Gaussian errors using a weighted least squares method that iteratively finds phase ambiguities for a GPS location solution using an *a posteriori* RMS error.

SUMMARY

[0013] A method for improving the results of radio location systems that incorporate weighted least squares optimization generalizes the weighted least squares method by using maximum *a posteriori* (MAP) probability metrics to incorporate characteristics of the specific positioning problem (e.g., UTDOA). As discussed, WLS methods are typically used by TDOA and related location systems including TDOA/AOA and TDOA/GPS hybrid systems. The incorporated characteristics include empirical information about TDOA errors and the probability distribution of the mobile position relative to other network elements. A technique is provided for modeling the TDOA error

distribution and the *a priori* mobile position. A method for computing a MAP decision metric is provided using the new probability distribution models.

[0014] An illustrative implementation provides an error detection method comprising: obtaining field data, wherein said field data have baseline or location dependent values to be used in said signal correlation model; analyzing said field data to obtain (1) a signal correlation model and associated measurement parameters, (2) correlation matrix rules, and (3) a model for *a priori* position; computing weights for the measurements based on an estimated variability of the measurement; using the weights along with the correlation matrix rules to generate a covariance matrix, and computing an inverse covariance matrix; performing an iterative search over a geographical region to find a location with a maximum *a posteriori* (MAP) metric; determining that a stopping condition has been reached; and reporting the geographic position with the largest MAP metric as the location solution.

[0015] The methods described herein include several key innovations, including but not necessarily limited to the following:

[0016] Analytical *a priori* distribution: Empirical data providing the actual locations are used to obtain a distribution for the normalized distance from the reference tower to the location solution in order to model the general shape of the *a priori* position relative to towers in the search area. An exponential distribution is shown to approximate the shape of the *a priori* position distribution and its variance is calculated from the empirical data.

[0017] Analytical TDOA error distribution: The double exponential distribution model is generalized to incorporate a skew and an arbitrary power in the exponent. Model parameters are estimated from empirical data.

[0018] Multipath/NLOS error indicators: Key indicators of the TDOA error distribution include the number of baselines, the predicted multipath correction (based on observed signal parameters and/or knowledge of the local RF environment) and the TDOA correlation of each baseline. Methods are provided to derive model parameters from these indicators by analyzing empirical data and generating conditional error distributions. For each baseline, model parameters such as the skew are computed from these indicators.

[0019] TDOA error correlation: Methods are provided for computing *a posteriori* probabilities for correlated errors between baselines that have the above analytical TDOA error distribution. These correlations are incorporated into the MAP algorithm through the corresponding joint error probability distribution.

[0020] Method for common bias mitigation: With more general distributions, it becomes difficult to find an analytical solution for the common bias that can exist in

measurements. Methods for removal of the bias are provided along with various complexity-performance tradeoffs.

[0021] Iterative adjustment: An iterative procedure is developed that applies the above methods. This procedure includes initialization operations and estimation of residual values.

[0022] Other features of the inventive technology are described below.

BRIEF DESCRIPTION OF THE DRAWINGS

[0023] The attached drawings include the following:

[0024] Figure 1: Illustration of a positioning network.

[0025] Figures 2a, 2b, 2c, and 2d: Illustration of impairments to LOS path delay estimation.

[0026] Figure 3: Illustration of causes for measurement error skewing.

[0027] Figures 4a and 4b: Components of MAP error detection method.

[0028] Figure 5: Error distribution modeling process.

[0029] Figure 6: Logic flow for the *a priori* distribution data analysis.

[0030] Figure 7: Comparison of *a priori* location distribution with empirical model.

[0031] Figure 8: Conditional error distribution data analysis.

[0032] Figure 9: Sample overall of error distribution vs. weighted least squares method.

[0033] Figure 10: Sample overall error distribution vs. new coarse model.

[0034] Figure 11: Sample dependency of skew ratio to correlation.

[0035] Figure 12: Sample overall conditional error distribution vs. new model (small skew).

[0036] Figure 13: Sample conditional error distribution vs. new model (large skew).

[0037] Figure 14: Logic flow of MAP decision metric computation.

[0038] Figure 15: Bias calculation for double exponential assumption (p=1,r=1).

[0039] Figure 16: Conditional error calculation.

DETAILED DESCRIPTION OF ILLUSTRATIVE EMBODIMENTS

[0040] Figures 4a-4b show the components of an illustrative implementation of the MAP error detection method. As shown, the MAP process is started at step 401. Field data 402 is analyzed 403 to obtain a set of signal correlation rules and models. These models and

associated measurement parameters are developed from field data that can have baseline or location (or position, where the terms *location* and *position* are used interchangeably herein) dependent values to be used in the model. For example, the error skew may be higher for low correlation UTDOA measurements. A table 405 may thus be generated. This table provides a mapping between the model parameter for the skew and the correlation value for the measurement. Similarly, a model and table is computed for the *a priori* location 406. The field data analysis process also analyzes the correlation between different receiver ports linking the location receiver (e.g., a Location Measuring Unit (LMU) or Signal Collection System (SCS)) to an external antenna, providing correlation values and rules for their application. For example, there may be small correlation of errors on ports at the same location (co-site ports) due to NLOS effects. Once the field data is analyzed, weights are computed for the measurements based on an estimated variability of the measurement. Then the weights are used along with the correlation matrix rules to generate a port by port covariance matrix, which is inverted at 409.

[0041] As shown in Figure 4b, an iterative search over a geographical region is then performed where the goal is to find the location with the largest MAP metric. Once the iterative search is initiated 411, a resolution loop is entered 412 in which the geographic search space resolution is reduced in each iteration and new test points are generated via interpolation. The search may be re-centered at the previous iteration's minimum error point before proceeding. The current geographical region is searched 414 by computing the MAP metric 415 for each test point in the region and selecting the point with the smallest metric. The MAP metric computation uses the covariance matrix 404, the error models and the measurement parameter tables 405. If more test points exist in the search space, the processing logic 417 loops back to restart the search 414. If no test points are untested in the present search space provided by the current resolution, the MAP process checks the pre-set resolution limit set 418. If the highest resolution has not been reached, the process returns to step 412; otherwise the MAP process checks if one or more stopping criteria has/have been reached 419. When the stopping criteria are met, the MAP process ends 420 and the geographic position with the largest metric provides the location solution.

[0042] A goal of our inventive solutions is to model the *a posteriori* probability of the error and find the location solution that maximizes this probability. From the Bayes theorem (see A. Papoulis, *Probability Random Variables, and Stochastic Processes*, McGraw

Hill Inc., New York, NY, 1984), the conditional probability density function of a random position vector, $\underline{L}$, is given in terms of a vector of N measurement errors, $\underline{e}$, as

$$f_{L|e}(\underline{L}|\underline{e}) = \frac{f_{e|L}(\underline{e}|\underline{L}) f_L(\underline{L})}{f_e(\underline{e})} \quad (1)$$

where,

$$\underline{L} \equiv \begin{bmatrix} x \\ y \\ z \end{bmatrix} \text{ is a random position vector} \quad (2)$$

$$\underline{e} = \begin{bmatrix} e_1 \\ e_2 \\ \dots \\ e_N \end{bmatrix} \equiv \begin{bmatrix} \hat{\tau}_1 - \tau_1(x,y,z) - B \\ \hat{\tau}_2 - \tau_2(x,y,z) - B \\ \dots \\ \hat{\tau}_N - \tau_N(x,y,z) - B \end{bmatrix} \text{ is the TDOA error plus a common bias} \quad (3)$$

and

$\tau_i(x,y,z)$ is the LOS TDOA at point x,y,z for the ith baseline,

$\hat{\tau}_i$ is the ith TDOA baseline measurement, and

B is a common bias that may exist in the measurements

[0043] To simplify computations, the log of (1) can be maximized since the position that maximizes (1) is also the position that maximizes the log of (1). The natural logarithm of (1) is

$$\ln\left(f_{L|e}(\underline{L}|\underline{e})\right) = \ln\left(f_{e|L}(\underline{e}|\underline{L})\right) + \ln\left(f_L(\underline{L})\right) - \ln\left(f_e(\underline{e})\right) \quad (4)$$

[0044] Since the last term does not depend on the location it is constant when considering different locations so it can be ignored. This leaves the following function to be maximized over all locations:

$$\ln\left(f_{L|e}(\underline{L}|\underline{e})\right) = \ln\left(f_{e|L}(\underline{e}|\underline{L})\right) + \ln\left(f_L(\underline{L})\right) \quad (5)$$

[0045] The first term is the log of the *a posteriori* error probability density and the second term is the log of the *a priori* probability density.

Error distribution modeling process

[0046] The error distribution modeling process is shown in Figure 5. Initially field data 402 is analyzed to determine the impact of various baseline and location specific measurement parameters on the *a priori* position distribution and the error distribution. Next, the correlation between errors for different baselines is analyzed to determine correlation

values and rules for obtaining these correlations. A coarse model for the error distribution 504 is found that fits the overall error distribution. A model for the *a priori* distribution is found based on the *a priori* distribution of the field data. The error distribution model is then refined in order to be modifiable based on the various location specific and baseline specific measurement parameters. Lastly, a correlation matrix is generated based on the correlation values and associated rules for applying the values.

A priori distribution

[0047] The logic for finding an appropriate *a priori* distribution is shown in Figure 6. Since location search areas can have vastly different dimensions depending on the location-specific data and location problems may also have vastly different network configurations, it is desirable to find a distribution of a model parameter that is a function of the actual position in the search area. The position in the search area is the *a priori* location. It is desirable to find a model parameter that is a function of the *a priori* location that can be computed and used to determine an *a priori* location probability for use in equation (5). Initially, the field data is analyzed to determine candidate parameters. For example, the statistics for the distance from a reference tower may be representative of the *a priori* location. Alternatively, the distance from a serving tower may be considered. These distances may be normalized to the maximum search range. For each parameter, the ranges and bin sizes must be chosen and histograms representing the *a priori* distribution updated based on the actual (true) location in the field data. Each potential distribution is stored along with the parameter computation in an *a priori* parameters database.

[0048] Once the potential *a priori* distributions are computed for various model parameters, a model is selected as depicted in Figure 5. The model is chosen to be both representative of the distribution from the field data and computationally efficient. An exemplary model parameter is chosen to be the distance of a candidate location from the reference tower normalized to the maximum distance from the reference tower to the edge of the search region. This provides a transformation from the three dimensional random vector, $\underline{L}$, to a normalized random distance from the reference tower, D, as

$$D = \frac{\left[\left(x - x_{ref}\right)^2 + \left(y - y_{ref}\right)^2 + \left(z - z_{ref}\right)^2\right]}{R_{\max}} \qquad (6)$$

where,

$x_{ref}, y_{ref}, z_{ref}$ are the position coordinates of the reference tower

R_{max} is the maximum distance from the reference tower to the edge of the search region.

An exemplary model is chosen to be exponential as

$$f_D(D) = \begin{cases} \lambda_a e^{-\lambda_a D} & x \geq 0 \\ 0 & \text{Otherwise} \end{cases} \quad (7)$$

where, $\lambda_a = 11$ was chosen to fit the field data. Figure 7 compares this model with the field data showing good agreement.

Error distribution

[0049] The field data is also analyzed to obtain models for the error distribution. Figure 8 shows a series of steps similar to those in the *a priori* data analysis. In the figure, measurement parameters are analyzed to determine which ones cause large changes in the error distribution. Exemplary measurement parameters include:

UTDOA correlation for each baseline,

Multipath correction factor for each baseline,

Number of measurements for each location.

[0050] Ranges and bin sizes for these parameters are determined for accumulating conditional and overall statistics. The conditional statistics and overall statistics are then compiled over all of the field data and stored for model determination.

[0051] A sample overall of error distribution is shown in Figure 9 and compared with the Gaussian distribution as would be assumed by weighted least squares methods. From the figure, it is evident that the Gaussian assumption does not adequately model the shape of the overall distribution. A skewing of the overall distribution to the right is apparent.

[0052] The overall distribution provides input to the coarse error model as shown in Figure 5. An exemplary error model for the ith marginal error is determined to be

$$f_{e_i|L}(x_i) = \begin{cases} Ae^{-\frac{k}{\sigma_i^{p_i}}|r_i x_i|^{p_i}} & x_i \geq 0 \\ Ae^{-\frac{k}{\sigma_i^{p_i}}\left|\frac{x_i}{r_i}\right|^{p_i}} & x_i < 0 \end{cases} \quad (8)$$

where,

p_i is a model parameter that is an arbitrary exponential power greater than zero,

r_i is a model parameter that is a positive ratio indicating the skew of the distribution, and

σ_i is the standard deviation for the ith baseline.

[0053] Values for k and A are chosen that satisfy the condition $\int_{-\infty}^{\infty} f_{e_i|L}(x)dx = 1$ for a given r_i and p_i. For a Gaussian distribution r_i=1, p_i=2 and k=1/2. For a double exponential distribution or Laplace distribution, r_i=1, p_i=1 and k=$\sqrt{2}$.

[0054] The coarse modeling step computes values for the model parameters in equation (8) that match the field data. Figure 10 illustrates the effects of applying the coarse model with p_i=1.1 and r_i=1.1. The figure shows significantly better agreement with the field data than the Gaussian assumption shown in Figure 9.

[0055] The conditional error distributions are used as input to the "determine fine error model" block 506 in Figure 5. For the conditional error, the skew ratio is computed based on the mean and standard deviation of the error for each measurement parameter bin. The center of the bin is the conditional value for the error distribution.

[0056] The skew can be found in terms of the mean and standard deviation of the conditional distribution as follows. If the conditional error distribution is approximated as a double exponential, then the scaling factor in the exponent is

$$\lambda = \sqrt{2}/\sigma \qquad (9)$$

where, σ is the standard deviation of the conditional distribution.

[0057] To estimate r_i, two separate scaled exponential distributions are considered where one of them is flipped around zero. Both components of the distribution are scaled to integrate to ½. As a result, the mean, m, of the conditional distribution can be put in terms of the scaling factors as

$$m = -\frac{1}{\lambda_L} + \frac{1}{\lambda_R} \qquad (10)$$

where, λ_L and λ_R are the scaling factors in the exponents of the separate exponential distribution components on the left and right of zero respectively. It is assumed that all of the skew is due to changes in λ_R relative to λ allowing for the assumption $\lambda_L \approx \lambda$. Solving equation (10) for λ_R and using (9) with $\lambda_L \approx \lambda$ gives

$$\lambda_R = \frac{1}{m + \frac{1}{\lambda_L}} \approx \frac{1}{m + \frac{\sigma}{\sqrt{2}}} \tag{11}$$

[0058] The skew ratio from (9) and (11) is then

$$r_i = \frac{\lambda_R}{\lambda_L} = \frac{\sigma}{\sqrt{2}m + \sigma} \tag{12}$$

[0059] Values for σ and m from the conditional error distribution can then be used to compute r_i using equation (12).

[0060] An example of the skew ratio as a function of the UTDOA correlation is shown in Figure 11. For each conditional distribution, the mean, m, and standard deviation, σ, are used in equation (12) to compute r_i. In the figure, it is evident that for low correlation, the skew increases. A linear fit to the data is shown which may be used in place of a table lookup to average out the variability that is a function of the number of samples and bin sizes. The result of the "fine error model determination" block 506 (Fig. 5) is a mapping of measurement parameter values, such as UTDOA correlation, to model parameters such as skew. Similar adjustments to the model parameter, p_i, in (8) can be made as a function of the various measurement parameter values.

[0061] Exemplary results of the fine model adjustments are shown in Figure 12 where there is a small skew at higher correlation. Figure 13 shows an example when there is a large skew at lower correlation. These figures illustrate that further improvement in the error distribution model is achieved relative to Figure 10.

Correlation matrix

[0062] The field data is also used to analyze the correlation that exists between errors for different ports as shown in Figure 5. The correlation between errors is computed based on various rules or conditions. Exemplary rules for computing the correlation between two ports include:

Apply a fixed correlation between ports on the same sector,

Apply a fixed correlation between ports on the same site,

Apply a fixed correlation between a cooperating port and the reference port.

[0063] For each rule a normalized correlation value or correlation coefficient for the error is computed from the field data statistics (see A. Papoulis, *Probability Random*

Variables, and Stochastic Processes, McGraw Hill Inc., New York, NY, 1984). The correlation values and rules provide input to the "populate covariance matrix and perform inversion" block 409 (Fig. 4a). The correlation matrix generation block computes a port by port matrix of correlation values. If multiple rules apply to a pair of ports then the largest correlation value is used in the matrix.

Weighting and Variance Computation

[0064] A weighting for each baseline is based on the RMS error from the Cramer Rao bound (see R. McDonough, A. Whalen, *Detection of Signals in Noise*, 2nd Ed., Academic Press., San Diego, CA, 1995). The lower bound on the TDOA RMS error in AWGN (additive white Gaussian noise) is

$$\sigma_i \approx \frac{\sqrt{12}\rho_i}{2\pi W(2WT)^{1/2}(1-\rho_i^2)^{1/2}} \tag{13}$$

where, W is the signal bandwidth, T is the coherent integration length and ρ_i is the correlation of the ith baseline. Since the mean error in AWGN is close to zero, the standard deviation of the error is approximately the RMS error. The weight is one over the RMS error squared, giving a theoretical weighting as

$$W_i = \frac{1}{\sigma_i^2} \tag{14}$$

[0065] These exemplary weighting operations are performed after the field data analysis in the "Compute Weights" block 407 as shown in Figure 4. Other effects may be included to account for degradations such as multipath which further increases the RMS error.

Covariance matrix computation

[0066] A covariance matrix may be required for making decisions using the joint error density. The covariance matrix, C, is a port by port matrix of the covariance between the ith and jth port which is computed as

$$c_{ij} = \beta_{ij}\sigma_i\sigma_j \tag{15}$$

where, β_{ij} is the correlation coefficient between the ith and jth port from the correlation matrix.

[0067] Alternatively this step may be bypassed for computational efficiency if the correlation levels between ports are deemed to be too small. An exemplary decision criterion

is to use the covariance matrix if at least one of the β_{ij} exceeds a correlation threshold. If this threshold is not exceeded a flag is set to use an independent error analysis.

MAP Decision Metric Computation

[0068] The MAP decision computation using the joint error density employs a further generalization for correlated UTDOA errors. Staring with joint Gaussian errors, the *a posteriori* probability is

$$\ln\left(f_{L|e}(\underline{L}|\underline{e})\right)=\ln\left(Ge^{-\frac{1}{2}\underline{e}C^{-1}\underline{e}^{T}}\right)=\ln(G)-\frac{1}{2}\underline{e}C^{-1}\underline{e}^{T} \tag{16}$$

where, G is a constant. In terms of the individual UTDOA errors

$$\ln\left(f_{L|e}(\underline{L}|\underline{e})\right)=\ln(G)-\frac{1}{2}\sum_{j}\sum_{i}e_{i}e_{j}d_{ij} \tag{17}$$

where, d_{ij} are elements of C^{-1}. Assuming the model in equation (8) for the marginal error probability density, the following generalization is made to equation (17) for the joint density,

$$\ln\left(f_{L|e}(\underline{L}|\underline{e})\right)=\ln(G)-k\sum_{j}\sum_{i}s_{ij}\left|h\left(r_{i},e_{i}\right)\right|^{p_{i}/2}\left|h\left(r_{j},e_{j}\right)\right|^{p_{j}/2}\left|d_{ij}\right|^{(p_{i}+p_{j})/4} \tag{18}$$

where,

$$h\left(r_{i},e_{i}\right)=\begin{cases}r_{i}e_{i} & e_{i}\geq 0\\ \dfrac{e_{i}}{r_{i}} & e_{i}<0\end{cases} \tag{19}$$

$$s_{ij}=\operatorname{sgn}\{h_{i}(r)\}\operatorname{sgn}\{h_{j}(r)\}\operatorname{sgn}\{d_{ij}\} \tag{20}$$

and

$$\operatorname{sgn}(x)=\begin{cases}1 & x>0\\ 0 & x=0\\ -1 & x<0\end{cases} \tag{21}$$

Substituting (18) and the natural log of (7) into (5) gives

$$\ln\left(f_{L|e}(\underline{L}|\underline{e})\right)=\ln(G)-k\sum_{j}\sum_{i}s_{ij}\left|h(r_{i},e_{i})\right|^{p_{i}/2}\left|h(r_{j},e_{j})\right|^{p_{j}/2}\left|d_{ij}\right|^{(p_{i}+p_{j})/4}+\ln(\lambda_{a})-\lambda_{a}D \tag{22}$$

[0069] Since the objective is to find the x,y,z and B that maximizes (22), the terms that do not depend on x,y,z and B can be ignored, giving:

$$\arg\max_{x,y,z,B}\left(\ln\left(f_{L|e}(\underline{L}|\underline{e})\right)\right)$$
$$=\arg\max_{x,y,z,B}\left(-k\sum_{j}\sum_{i}s_{ij}\left|h(r_i,e_i(x,y,z))\right|^{p_i/2}\left|h(r_j,e_j(x,y,z))\right|^{p_j/2}\left|d_{ij}\right|^{(p_i+p_j)/4}-\lambda_a D(x,y,z)\right) \quad (23)$$

[0070] For computational efficiency, equation (23) may be divided by -k and the x,y,z that minimizes $-\frac{1}{k}\ln\left(f_{L|e}(\underline{L}|\underline{e})\right)$ is found as

$$\arg\max_{x,y,z,B}\left(\ln\left(f_{L|e}(\underline{L}|\underline{e})\right)\right)=\arg\min_{x,y,z,B}\left(-\frac{1}{k}\ln\left(f_{L|e}(\underline{L}|\underline{e})\right)\right)$$
$$=\arg\min_{x,y,z,B}\left(\sum_{j}\sum_{i}s_{ij}\left|h\ (r_i,e_i(x,y,z,B))\right|^{p_i/2}\left|h\ (r_j,e_j(x,y,z,B))\right|^{p_j/2}\left|d_{ij}\right|^{(p_i+p_j)/4}+\frac{\lambda_a}{k}D(x,y,z)\right) \quad (24)$$

[0071] The decision metric to be minimized is then

$$M=\sum_{j}\sum_{i}s_{ij}\left|h(r_i,e_i(x,y,z,B))\right|^{p_i/2}\left|h(r_j,e_j(x,y,z,B))\right|^{p_j/2}\left|d_{ij}\right|^{(p_i+p_j)/4}+\frac{\lambda_a}{k}D(x,y,z)$$

(25)

[0072] For locations where there is low (~0) cross-correlation between baselines, the covariance matrix is diagonal. Independence is assumed between UTDOA errors simplifying (25) to

$$M=\sum_{i}\frac{1}{\sigma_i^p}\left|h(r_i,e_i(x,y,z,B))\right|^{p_i}+\frac{\lambda_a}{k}D(x,y,z) \quad (26)$$

[0073] In terms of the pre-computed weights for each baseline, the metric is

$$M=\sum_{i}W_i^{p_i/2}\left|h(r_i,e_i(x,y,z,B))\right|^{p_i}+\frac{\lambda_a}{k}D(x,y,z) \quad (27)$$

[0074] Figure 14 shows the logic flow for the MAP decision metric computation at each x,y,z value. The error samples are computed for the x,y,z being considered 1401. In general, an analytical solution for the common bias, "B", in equation (27) that minimizes M is difficult to compute. Therefore, the biases at two relatively easy to compute sample points (p_i=1, r_i=1 and p_i=2, r_i=1) are found and combined to provide an approximation. A minimum bias is computed assuming Gaussian statistics 1402 for the errors followed by a computation assuming double exponential statistics 1403. The bias to be used is then found by combining the two bias points 1404. The combining can be done by simply taking the

average of the Gaussian and double exponential biases. Alternatively, the bias for arbitrary p_i and r_i can be found through a search over all possible biases at the cost of complexity. If this is done, the average of the two bias samples is used as a starting point for the search. Alternatively, the search can be done offline and compared with the bias results for the two bias samples. In this case, the average percentage deviation from the two bias points may be used in the combining at the cost of offline analysis. After combining the sample biases, the conditional error contribution is determined 1405 using the combined bias 1405, the covariance matrix 1407, and the Error Model and Parameter table as previously developed from the field data. The computed conditional error contribution 1405 and the previously developed Model for A Priori Position 1409 are then used to find an *a priori* contribution 1406 to the MAP metric. The minimum of the metric computation in Figure 14 over x,y,z with various geographical map resolutions and iterations provides the final solution as depicted in Figure 4.

Gaussian Bias

[0075] The Gaussian bias is found by setting p_i=2 and r_i=1 in (27). Note that for r_i=1,

$h(r_i = 1, e_i(x, y, z, B)) = e_i(x, y, z, B)$ giving

$$M = \sum_{i=1}^{N} (\Delta\tau_i - B)^2 W_i \qquad (28)$$

where,

N is the number of baselines

$\Delta\tau_i \equiv \hat{\tau}_i - \tau_i(x, y, z)$ is the unbiased error.

[0076] A minimum solution over the bias is found by setting the derivative of (28) with respect to B equal to zero and solving for B giving

$$B = \sum_{i=1}^{N} \Delta\tau_i W_i \Big/ \sum_{i=1}^{N} W_i . \qquad (29)$$

Equation (29) provides a bias when the error distributions are Gaussian.

Exponential Bias

[0077] The exponential bias is found by setting p_i=1 and r_i=1 in (27) giving

$$M = \sum_{i=1}^{N} |\Delta\tau_i - B| \sqrt{W_i} \tag{30}$$

[0078] Again, a minimum solution over the bias is found by setting the derivative of (28) with respect to B equal to zero and solving for B. The derivative of each term with respect to B is

$$\begin{aligned} \frac{d}{dB}|\Delta\tau_i - B|\sqrt{W_i} &= \begin{cases} \sqrt{W_i} & B \geq \Delta\tau_i \\ -\sqrt{W_i} & B < \Delta\tau_i \end{cases} \\ &= \sqrt{W_i}\left[U(B-\Delta\tau_i) - U(\Delta\tau_i - B)\right] \end{aligned} \tag{31}$$

where, U(x) is a unit step function (see A. Oppenhem and A. Willsky, *Signals and Systems*, Prentice-Hall, Inc., Englewood Cliffs, NJ, 1983). Setting the derivative of the sum equal to zero gives

$$\frac{dM}{dB} = \sum_{i=1}^{N} \sqrt{W_i}\left[U(B-\Delta\tau_i) - U(\Delta\tau_i - B)\right] = 0 \tag{32}$$

[0079] Each term in (32) as a function of B is $-\sqrt{W_i}$ until the value $\Delta\tau_i$ is reached and then there is a step to $\sqrt{W_i}$ for B greater than $\Delta\tau_i$. Due to these discontinuities, there is no exact solution for B. However, a value for B can be found that provides an approximate solution.

[0080] A solution in Figure 15 orders the summation in (32) according to increasing $\Delta\tau_i$. The value of B is then found that makes (32) as close as possible to zero. This occurs at a value of B where the kth step transition has occurred making the sum of the negative terms approximately equal to the sum of the positive terms (i.e. $\sum_{i=1}^{K} \sqrt{W_i} \approx -\sum_{i=K+1}^{N} \sqrt{W_i}$ where N is the total number of baselines in the ordered summation). In the figure the weight and sample arrays are populated and sorted. A threshold is computed that is $\sum_{i=1}^{N} \sqrt{W_i} \Big/ 2$ to provide a stopping condition. The terms are accumulated in order from the terms with the smallest to the largest transition point. At the point where the threshold is reached, the value $\Delta\tau_K$ is returned if there are an odd number of terms; otherwise, the kth term's transition point is averaged with the prior term's transition point.

Metric Calculation

[0081] The first term in (27) is computed following the steps in Figure 16. For each baseline, the measurement parameters such as UTDOA correlation, the number of baselines and multipath parameters are determined. These measurement parameters are used to determine error model parameters, p_i and r_i, from a lookup table or through a direct calculation using a parameter fitting model. The errors are adjusted depending on the skew. Finally, the summation in the metric is computed using (25) when the errors have significant correlation or using (27) when the errors do not have significant correlation. The significance of the correlation is determined as part of the covariance matrix computations in Figure 4. Finally, the last term in (27) and (25) is computed using (6) to account for the *a priori* probability.

Sample Results

[0082] Table 1 below illustrates sample improvements relative to a weighted least squares algorithm. Using approximately 46,000 location measurements, the distribution of positioning errors were compiled using the weighted least squares algorithm and the algorithm above. The parameters for the above model were chosen using a separate training data set of 32,000 locations. The table shows improvement of approximately 20 meters and 2 meters in the 95th and 67th percentiles respectively. The average error improved by approximately 15 meters.

Error (m)	Weighted Least Squares	MAP
67th percentile	74.7	72.9
95th percentile	293.1	271.3
Average	287.9	272.6

Table 1: Exemplary Results Relative to Weighted Least Squares Method

Conclusion

[0083] The present invention, and the scope of protection of the following claims, is by no means limited to the details described hereinabove. Those of ordinary skill in the field of wireless location will appreciate that various modifications may be made to the illustrative embodiments without departing from the inventive concepts disclosed herein.

What is Claimed:

1. An error detection method, comprising:

obtaining field data (402), wherein said field data have baseline or location dependent values to be used in said signal correlation model;

analyzing said field data (403) to obtain (1) a signal correlation model and associated measurement parameters (405), (2) correlation matrix rules (404), and (3) a model for *a priori* position (406);

computing weights (407) for the measurements based on an estimated variability of the measurement;

using the weights along with the correlation matrix rules to generate a covariance matrix (409), and computing an inverse covariance matrix (410);

performing an iterative search over a geographical region to find a location with a maximum *a posteriori* (MAP) metric (415);

determining that a stopping condition has been reached (419); and

reporting the geographic position with the largest MAP metric as the location solution.

2. A method as recited in claim 1, further comprising generating a table providing a mapping between the measurement parameters for a skew and a correlation value for the measurement.

3. A method as recited in claim 1, further comprising generating a table providing a mapping between the measurement parameters for a skew and the number of baselines.

4. A method as recited in claim 1, wherein further comprising analyzing the correlation between different receiver ports linking the location receiver to an external antenna, providing correlation values and rules for their application.

5. A method as recited in claim 1, wherein said iterative search includes a resolution loop in which a geographic search space resolution is reduced in each iteration and new test points are generated via interpolation.

6. A method as recited in claim 5, wherein the search is re-centered at the previous iteration's minimum error point before proceeding, wherein test points within the current geographical region search space are individually searched and a MAP metric is computed for each test point.

7. A method as recited in claim 1, wherein the iterative search includes a MAP metric computation that uses the covariance matrix, error model and measurement parameter table.

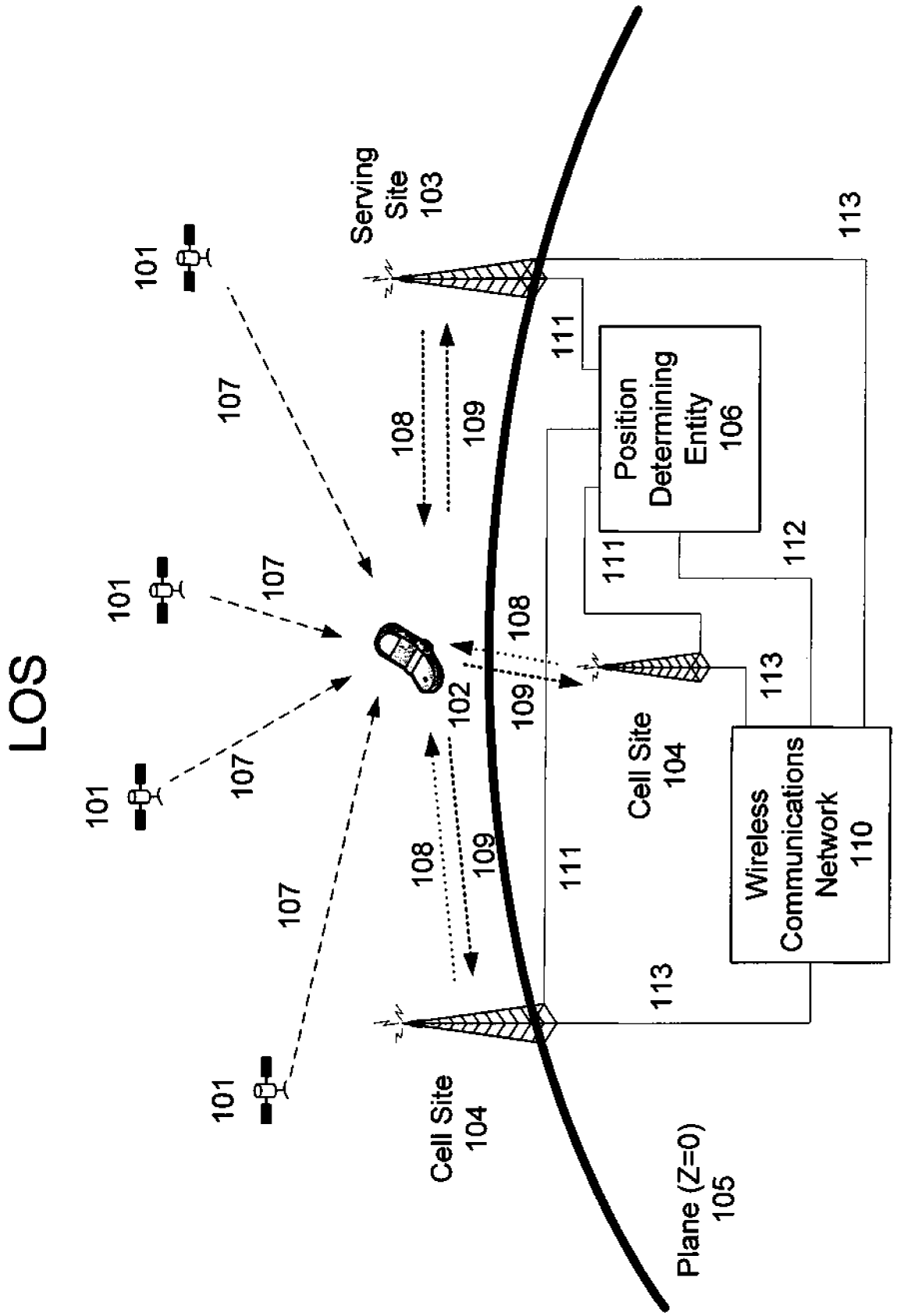
LOS
101
107
Serving Site 103
108
109
111
Position Determining Entity 106
112
113
102
Cell Site 104
Wireless Communications Network 110
Plane (Z=0) 105

Figure 1

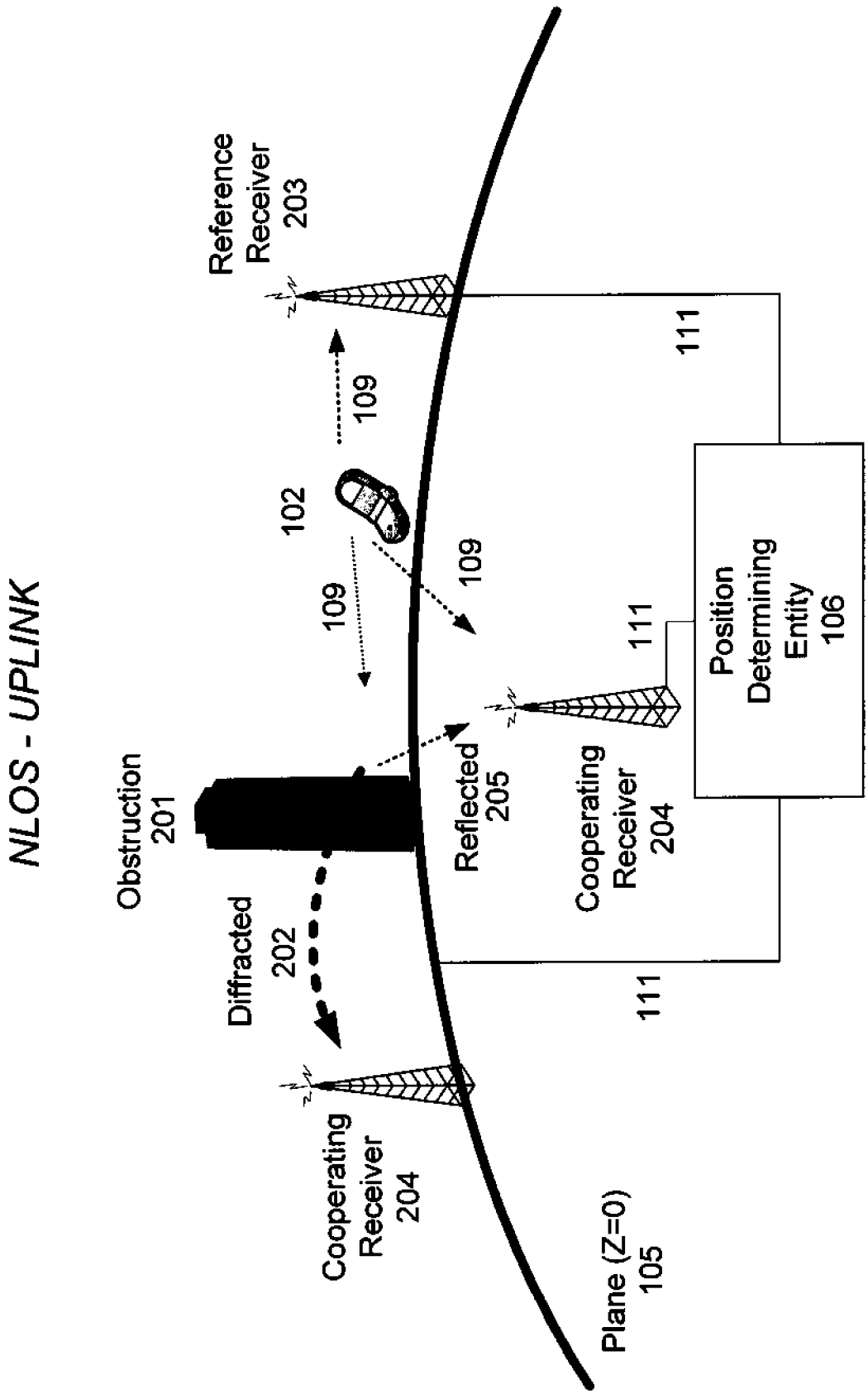
NLOS - UPLINK
Reference Receiver 203
102
109
109
109
111
Position Determining Entity 106
111
Obstruction 201
Diffracted 202
Reflected 205
Cooperating Receiver 204
Cooperating Receiver 204
111
Plane (Z=0) 105

Figure 2

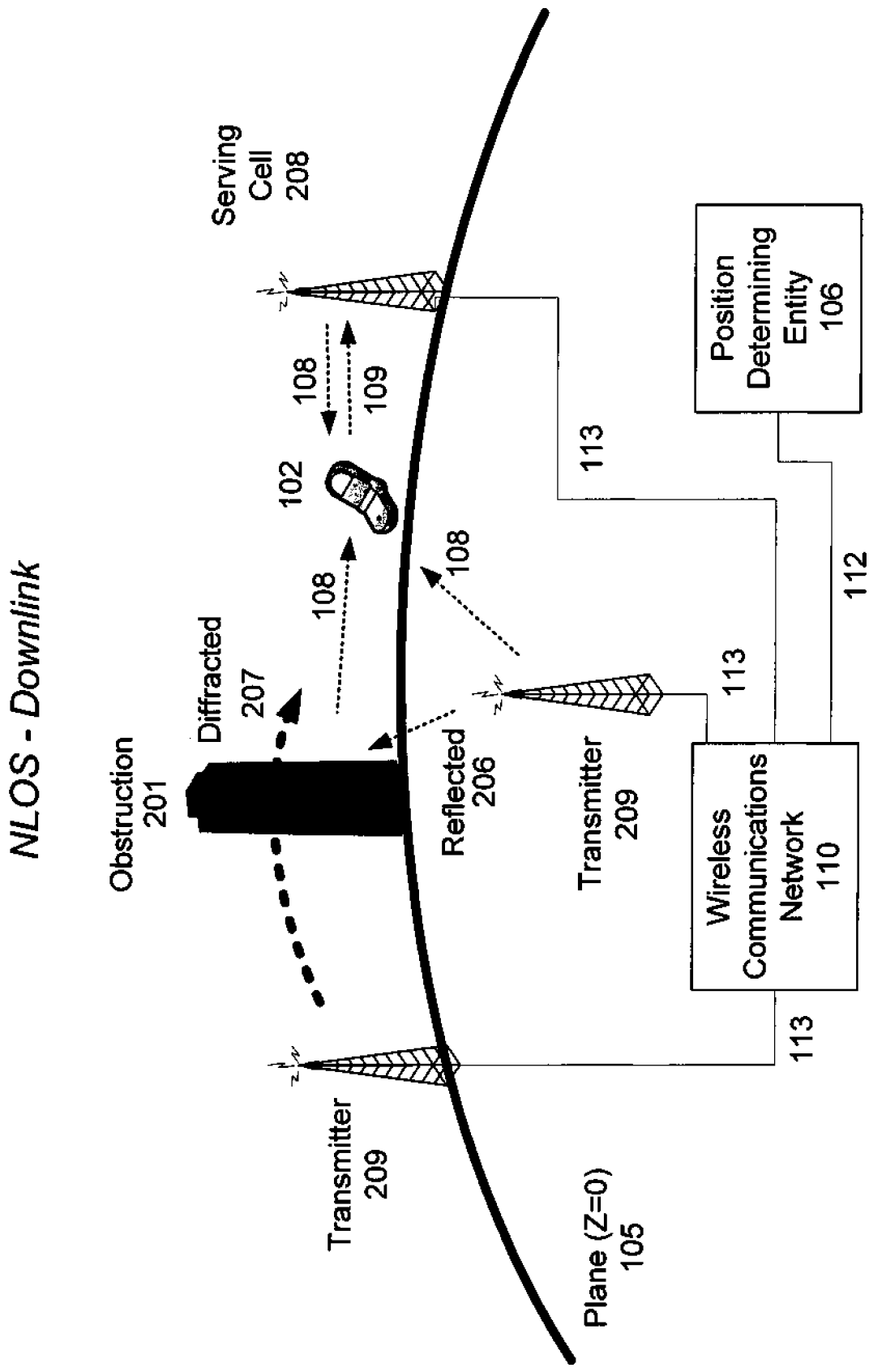
NLOS - Downlink
Serving Cell 208
Position Determining Entity 106
113
112
102
108
109
108
108
Diffracted 207
Obstruction 201
Reflected 206
Transmitter 209
113
Wireless Communications Network 110
113
Transmitter 209
Plane (Z=0) 105

Figure 2b

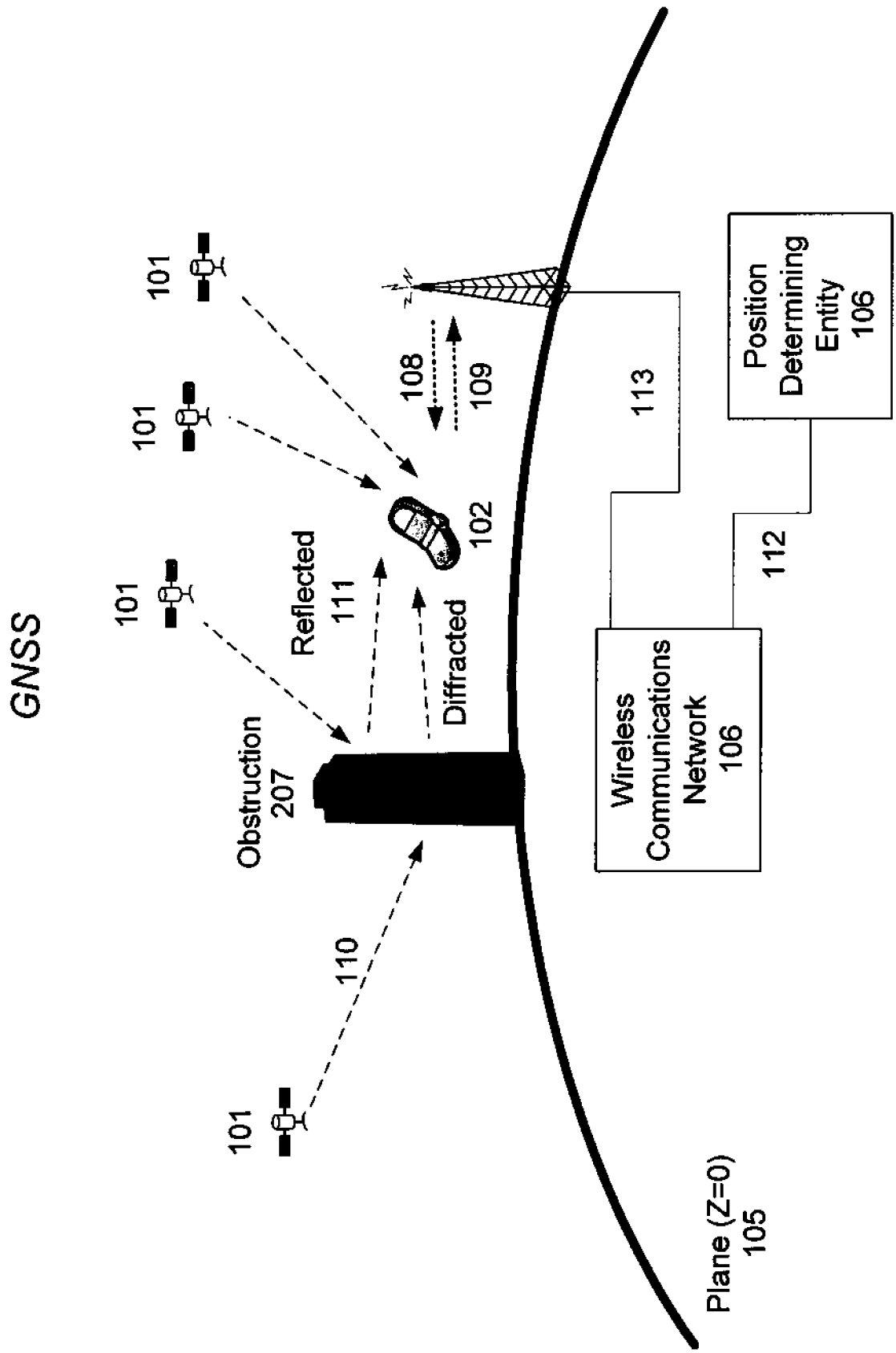
GNSS
101
101
101
101
101
Obstruction
207
Reflected
111
Diffracted
108
109
102
110
113
112
Position
Determining
Entity
106
Wireless
Communications
Network
106
Plane (Z=0)
105

Figure 2c

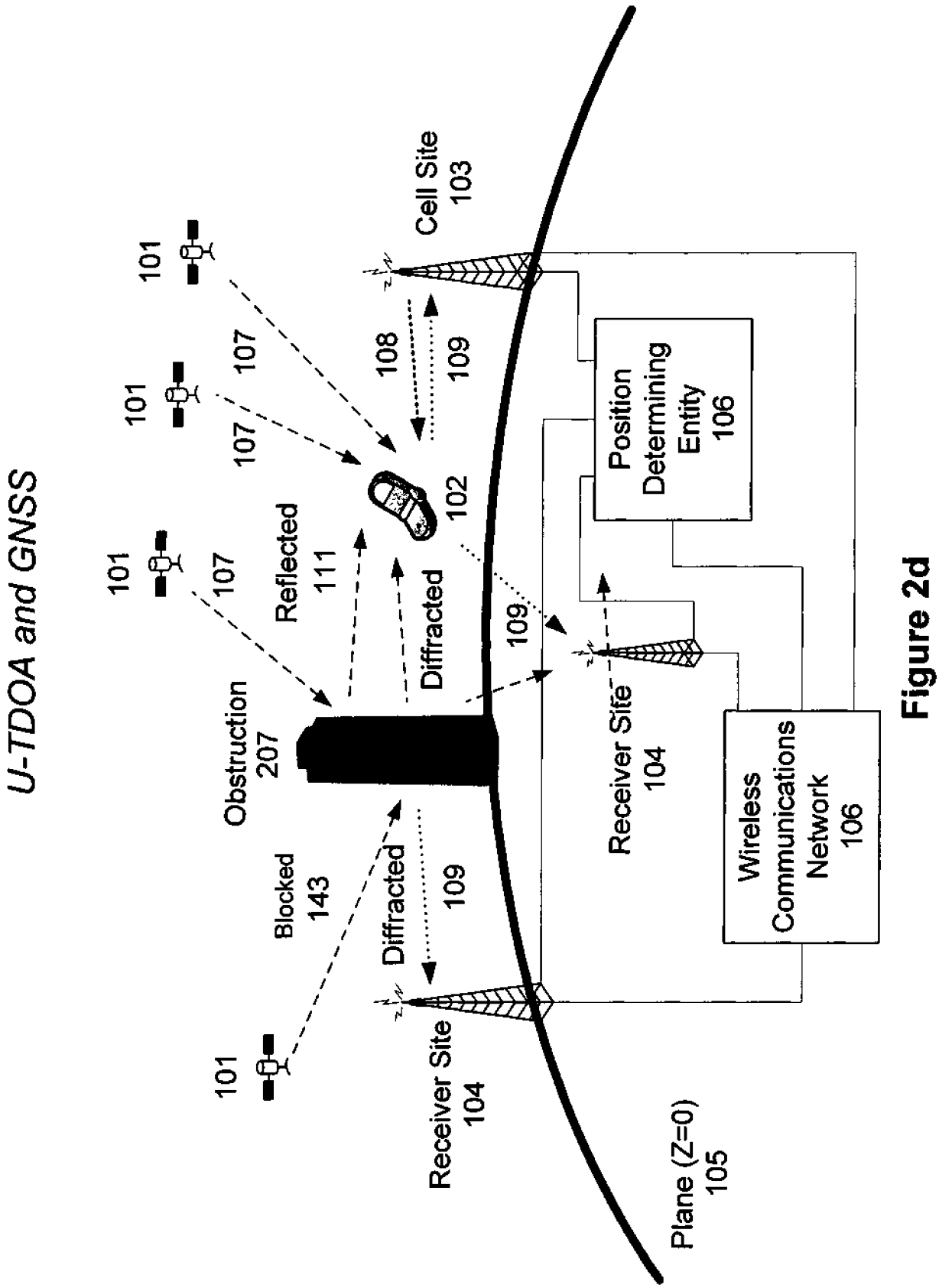
U-TDOA and GNSS
Cell Site
103
101
107
108
109
Position
Determining
Entity
106
102
Reflected
111
Diffracted
Obstruction
207
Receiver Site
104
Wireless
Communications
Network
106
Blocked
143
Receiver Site
104
Plane (Z=0)
105

Figure 2d

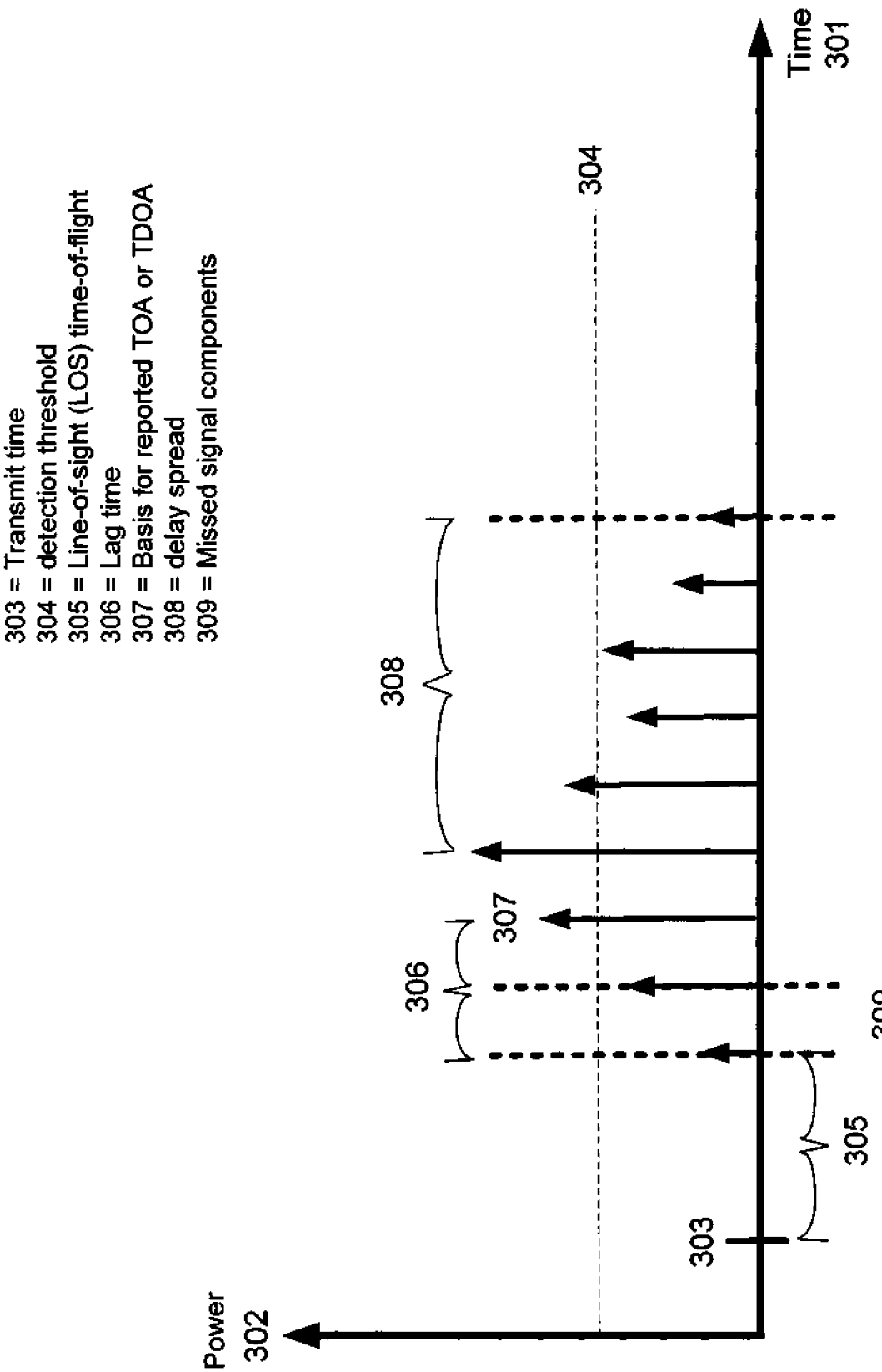
303 = Transmit time
304 = detection threshold
305 = Line-of-sight (LOS) time-of-flight
306 = Lag time
307 = Basis for reported TOA or TDOA
308 = delay spread
309 = Missed signal components
Power
302
Time
301
303
304
305
306
307
308
309

Figure 3

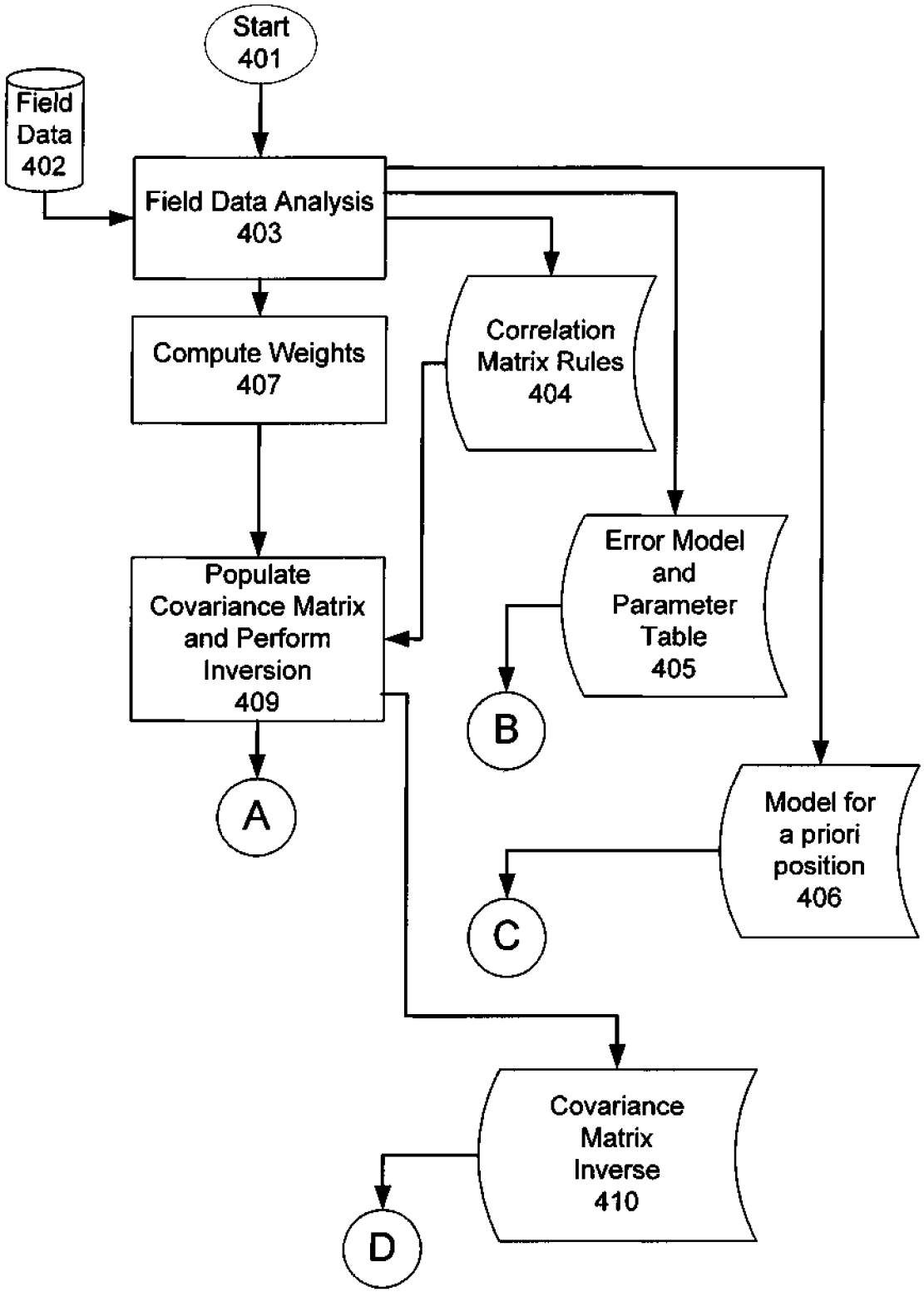
Start
401
Field
Data
402
Field Data Analysis
403
Compute Weights
407
Correlation
Matrix Rules
404
Error Model
and
Parameter
Table
405
Populate
Covariance Matrix
and Perform
Inversion
409
B
A
Model for
a priori
position
406
C
Covariance
Matrix
Inverse
410
D

Figure 4a

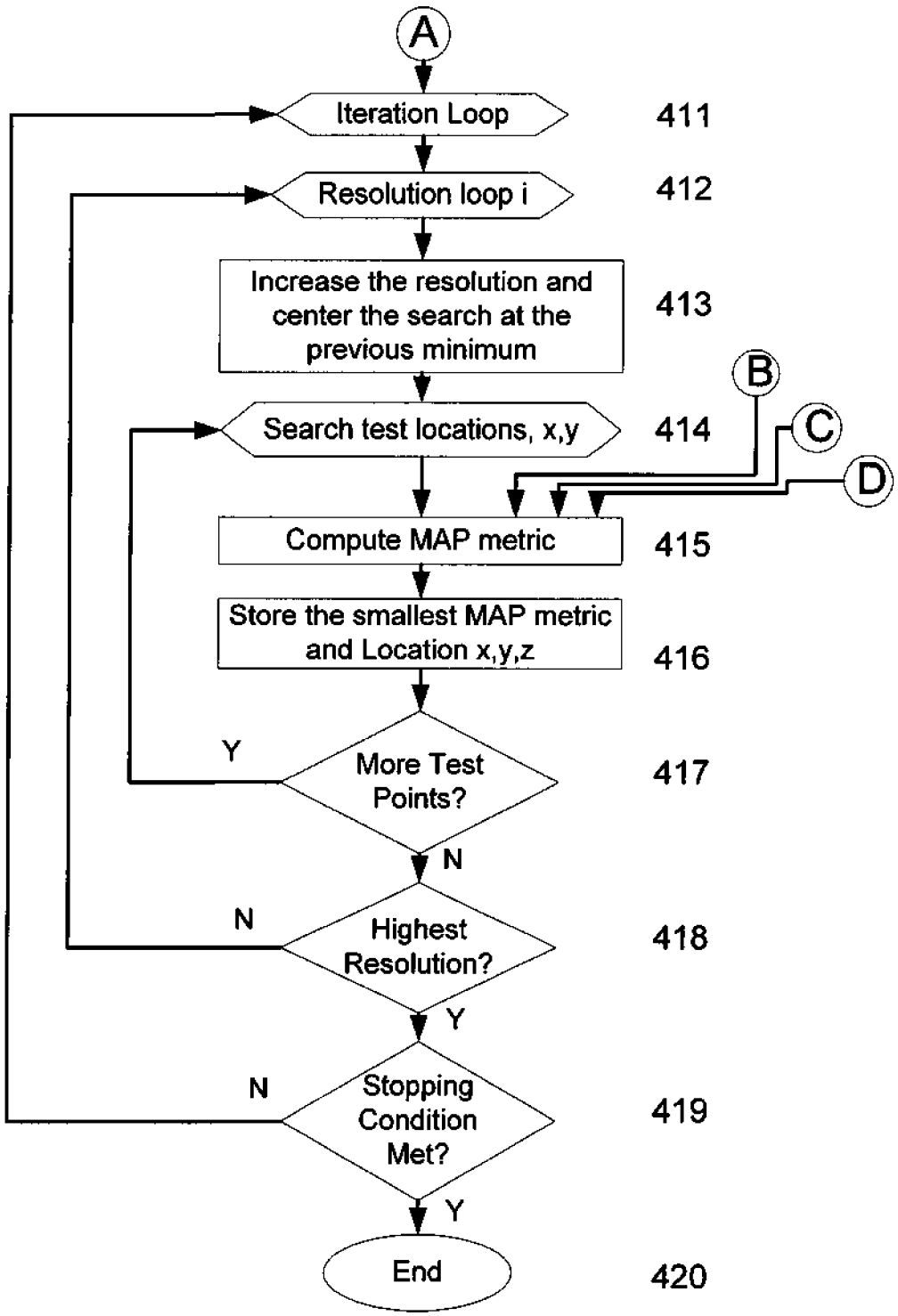
A
Iteration Loop
411
Resolution loop i
412
Increase the resolution and center the search at the previous minimum
413
B
C
D
Search test locations, x,y
414
Compute MAP metric
415
Store the smallest MAP metric and Location x,y,z
416
Y
More Test Points?
417
N
N
Highest Resolution?
418
Y
N
Stopping Condition Met?
419
Y
End
420

Figure 4b

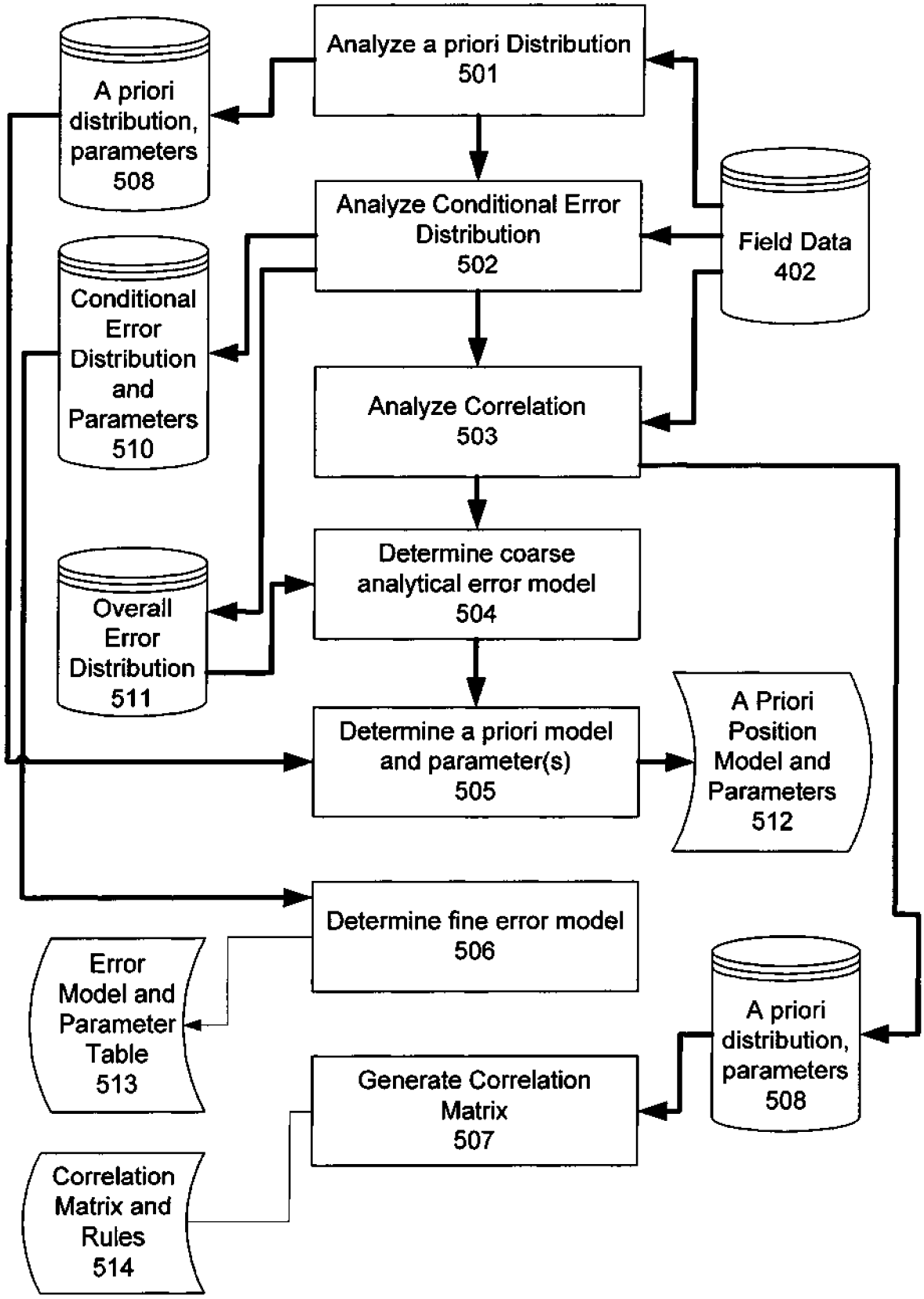
Analyze a priori Distribution
501
A priori distribution, parameters
508
Analyze Conditional Error Distribution
502
Field Data
402
Conditional Error Distribution and Parameters
510
Analyze Correlation
503
Determine coarse analytical error model
504
Overall Error Distribution
511
Determine a priori model and parameter(s)
505
A Priori Position Model and Parameters
512
Determine fine error model
506
Error Model and Parameter Table
513
A priori distribution, parameters
508
Generate Correlation Matrix
507
Correlation Matrix and Rules
514

Figure 5

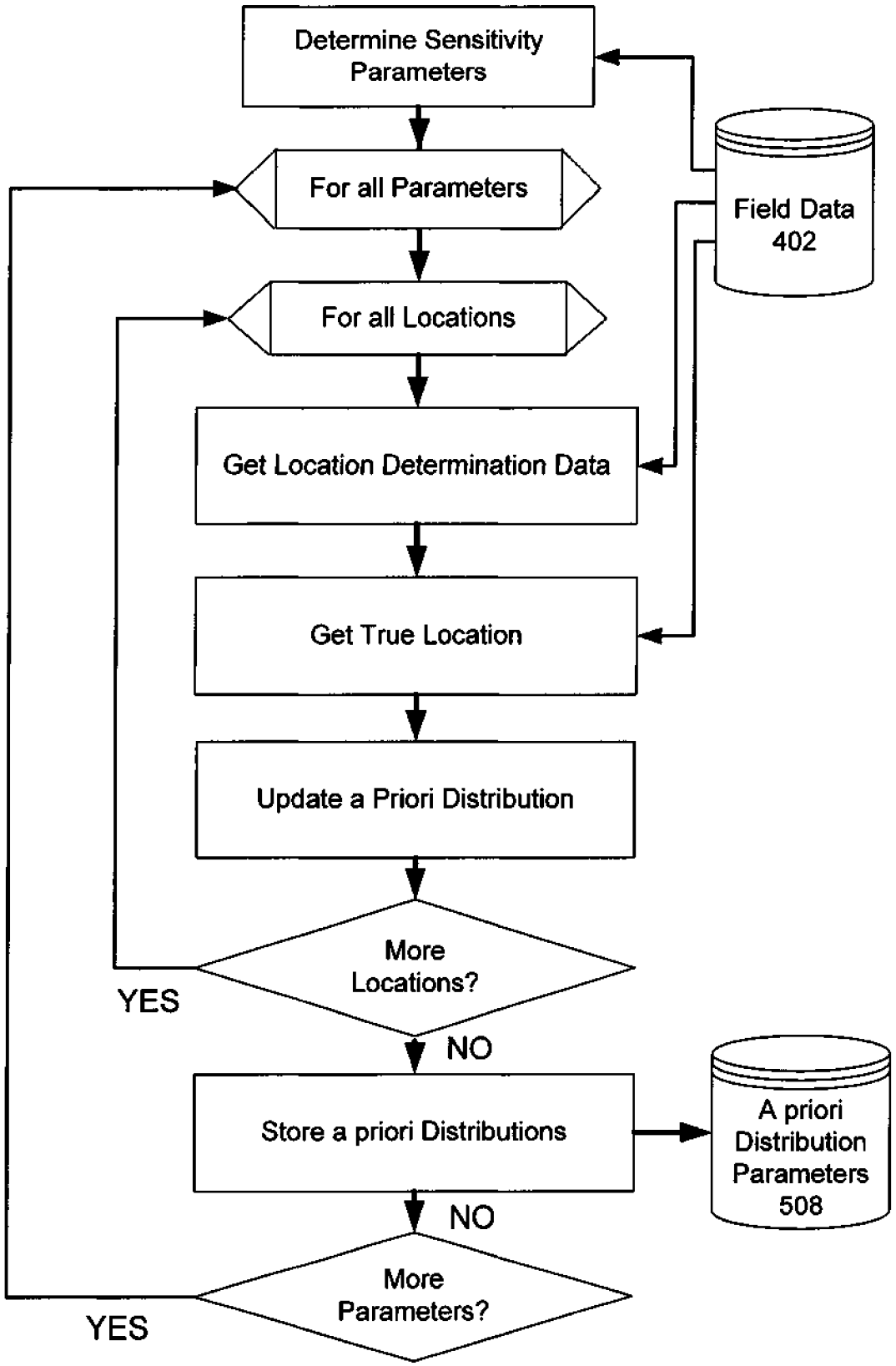
Determine Sensitivity Parameters
For all Parameters
For all Locations
Get Location Determination Data
Get True Location
Update a Priori Distribution
More Locations?
YES
NO
Store a priori Distributions
More Parameters?
YES
NO
Field Data 402
A priori Distribution Parameters 508

Figure 6

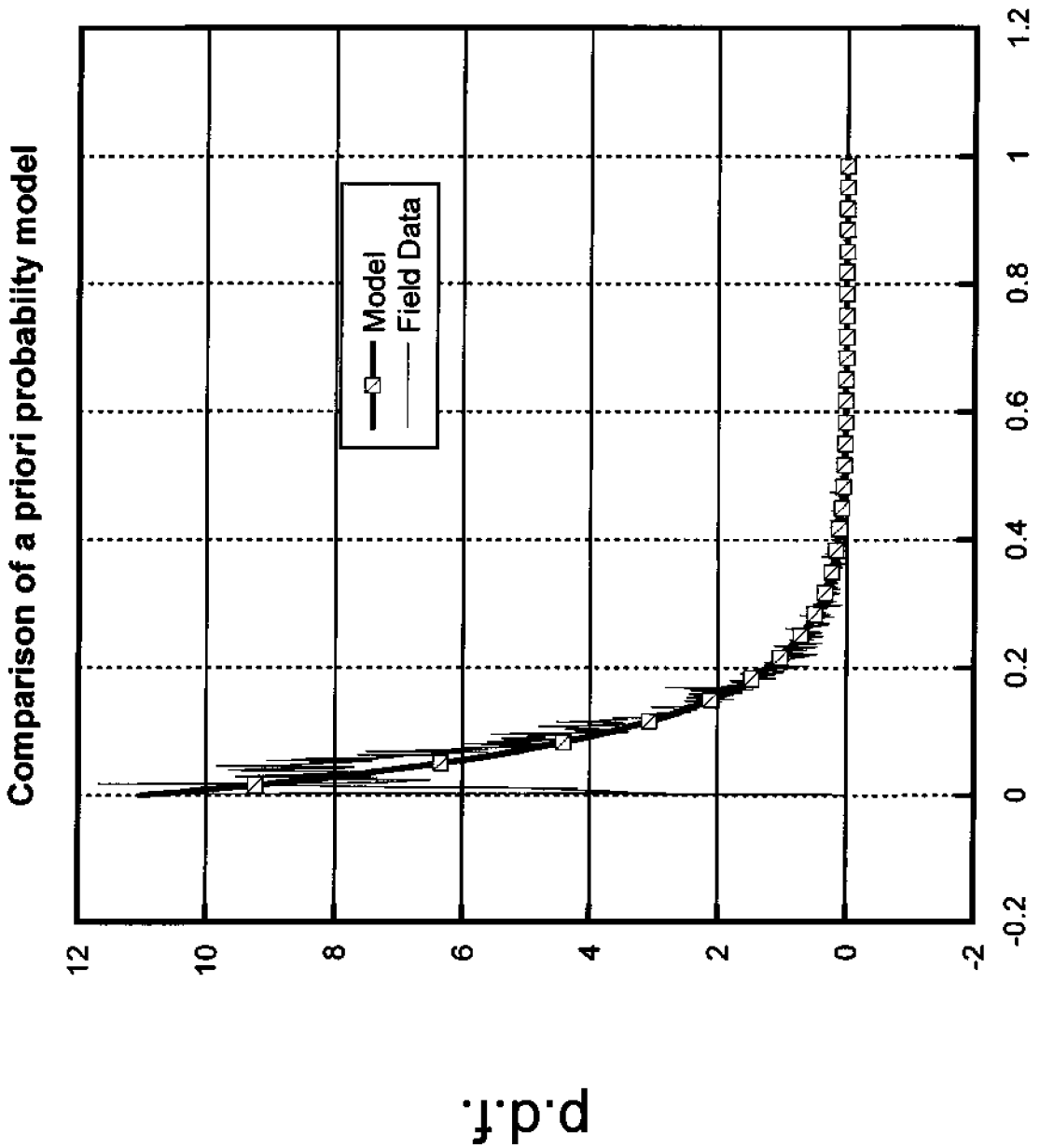
Comparison of a priori probability model
Model
Field Data
p.d.f.
12
10
8
6
4
2
0
-2
-0.2
0
0.2
0.4
0.6
0.8
1
1.2
Normalized Distance

Figure 7

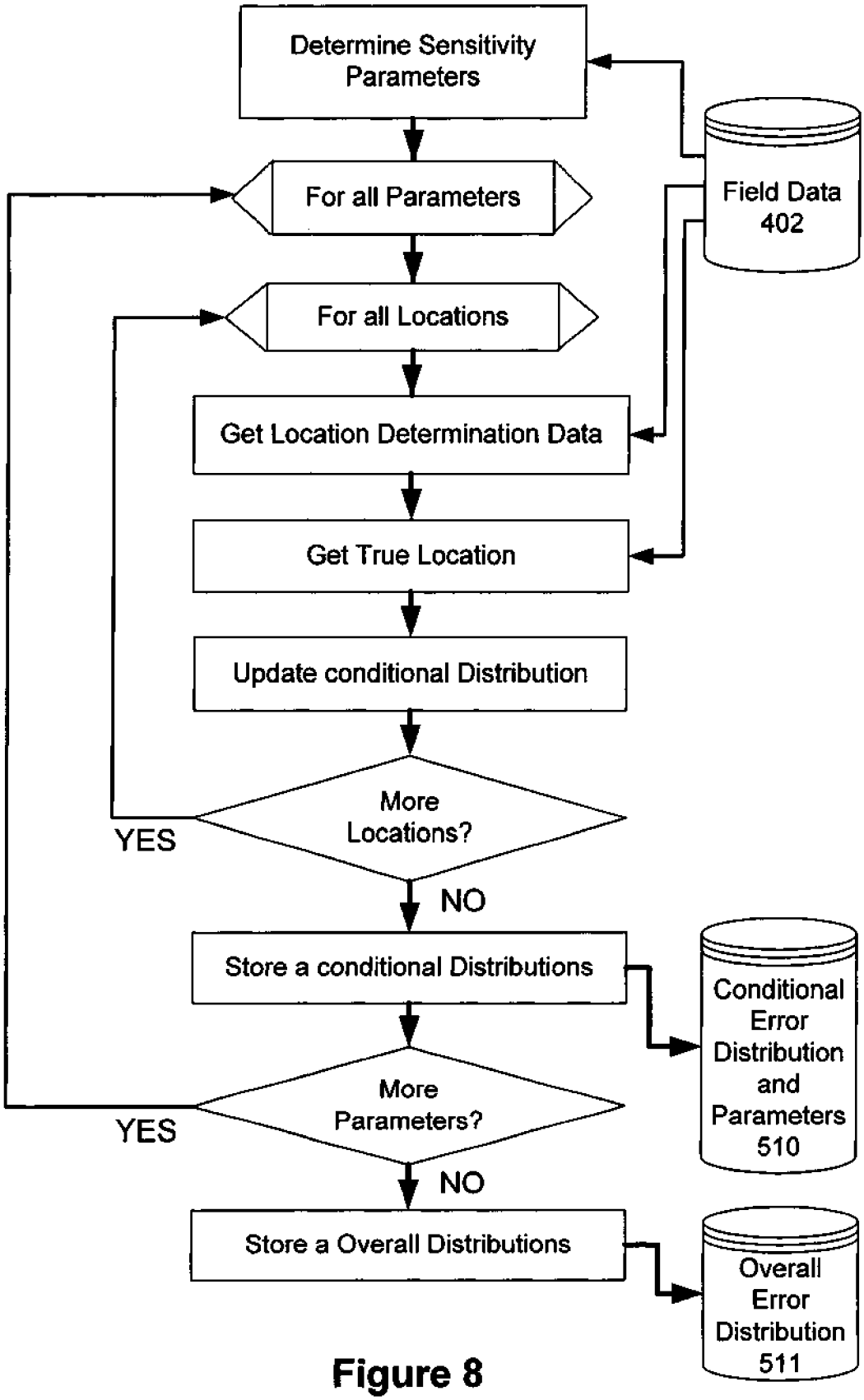
Determine Sensitivity Parameters
For all Parameters
For all Locations
Get Location Determination Data
Get True Location
Update conditional Distribution
More Locations?
YES
NO
Store a conditional Distributions
More Parameters?
YES
NO
Store a Overall Distributions
Field Data 402
Conditional Error Distribution and Parameters 510
Overall Error Distribution 511

Figure 8

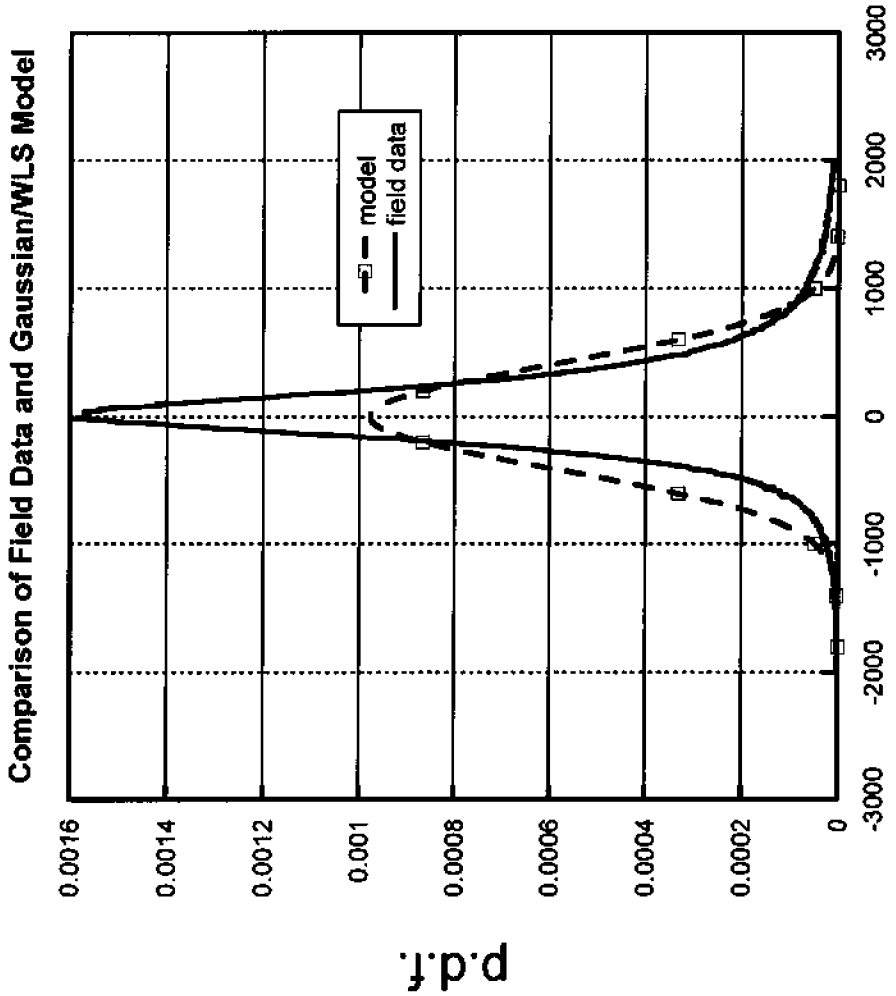
Comparison of Field Data and Gaussian/WLS Model
model
field data
p.d.f.
0.0016
0.0014
0.0012
0.001
0.0008
0.0006
0.0004
0.0002
0
-3000
-2000
-1000
0
1000
2000
3000
TDOA Error (ns)

Figure 9

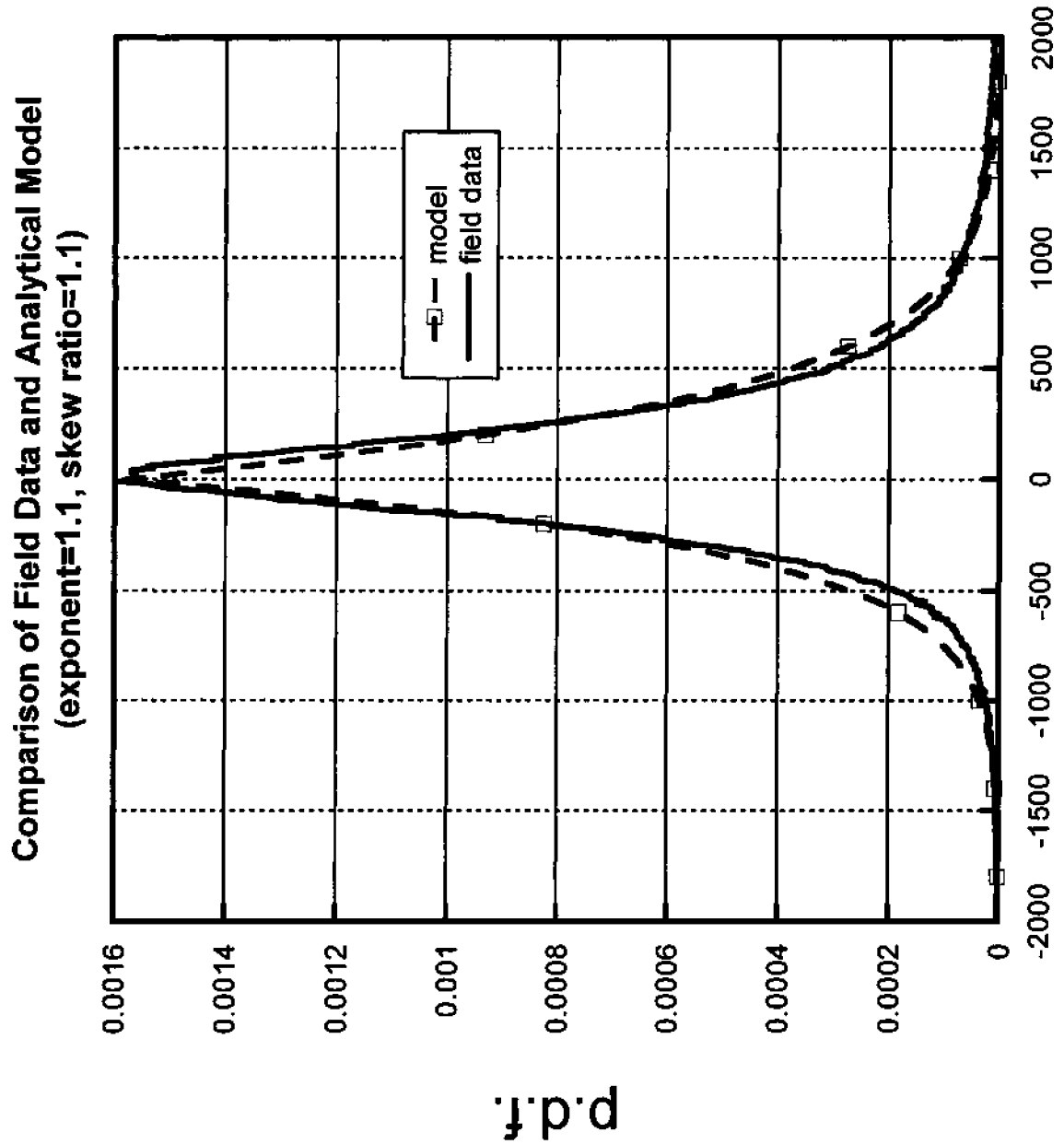
Comparison of Field Data and Analytical Model
(exponent=1.1, skew ratio=1.1)
model
field data
p.d.f.
0.0016
0.0014
0.0012
0.001
0.0008
0.0006
0.0004
0.0002
0
-2000
-1500
-1000
-500
0
500
1000
1500
2000
TDOA Error (ns)

Figure 10

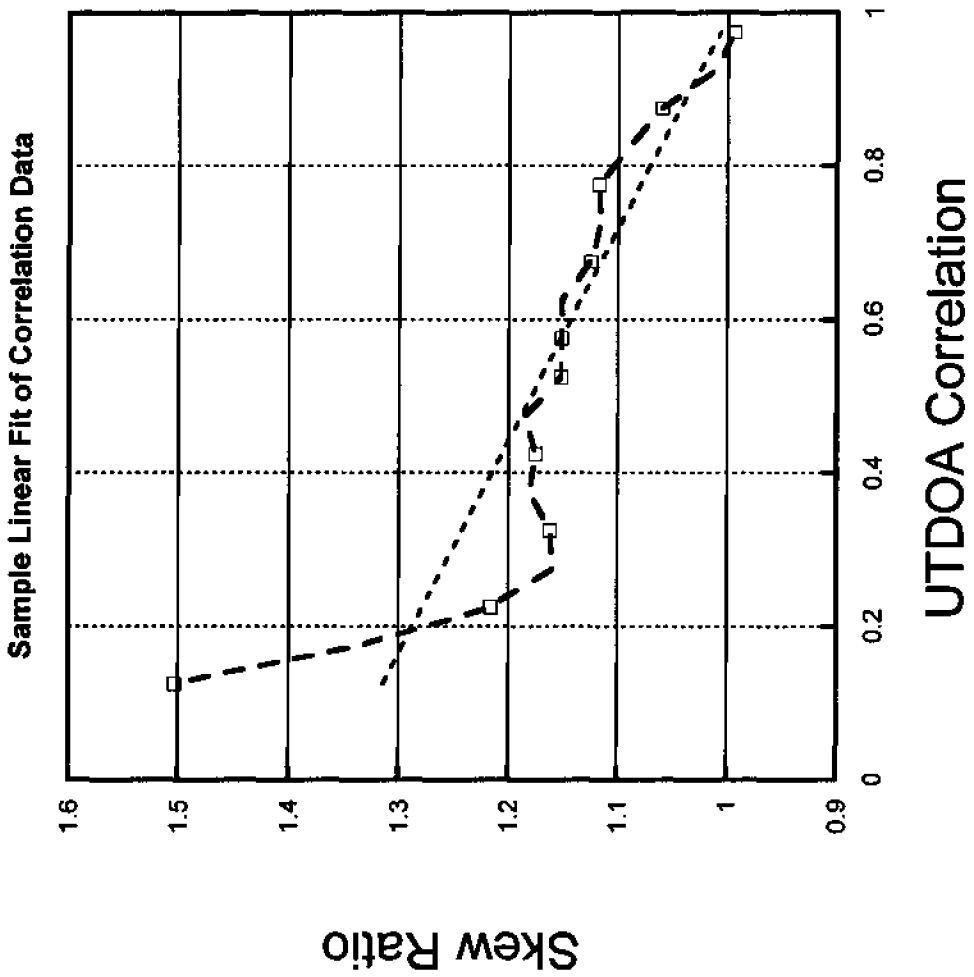
Sample Linear Fit of Correlation Data
Skew Ratio
UTDOA Correlation
1.6
1.5
1.4
1.3
1.2
1.1
1
0.9
0
0.2
0.4
0.6
0.8
1

Figure 11

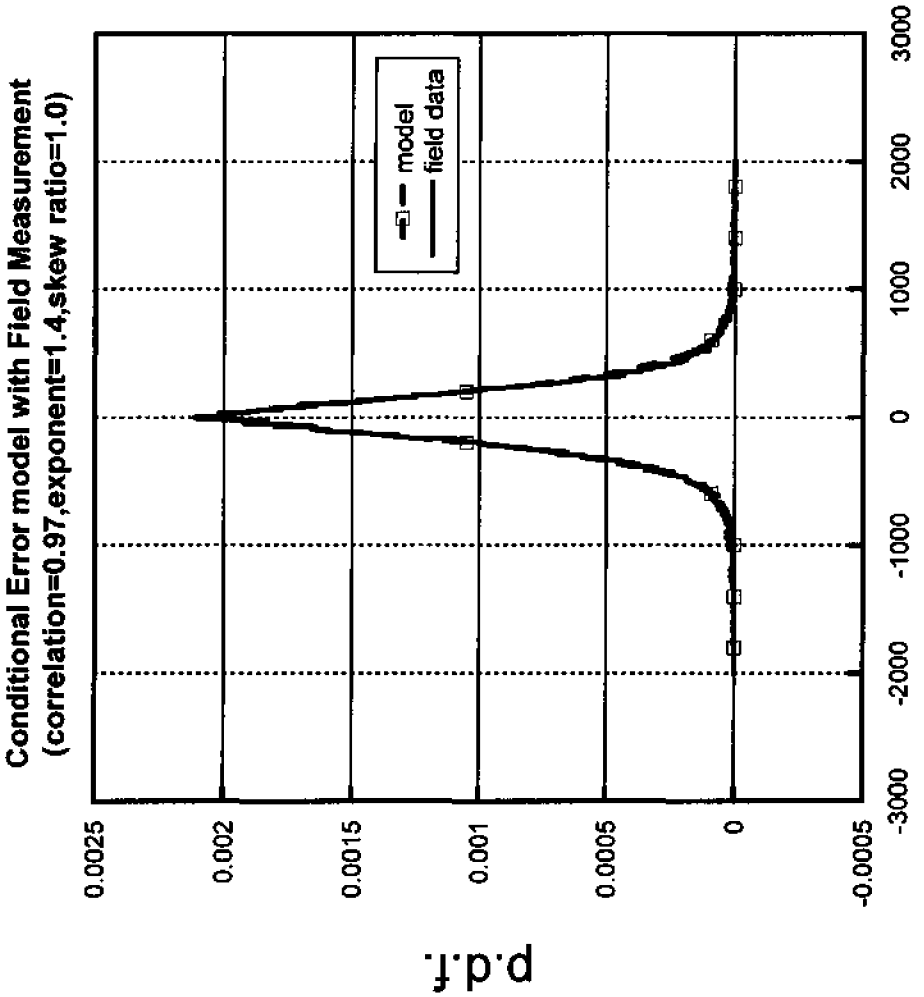
Conditional Error model with Field Measurement
(correlation=0.97,exponent=1.4,skew ratio=1.0)
model
field data
p.d.f.
0.0025
0.002
0.0015
0.001
0.0005
0
-0.0005
-3000
-2000
-1000
0
1000
2000
3000
TDOA Error (ns)

Figure 12

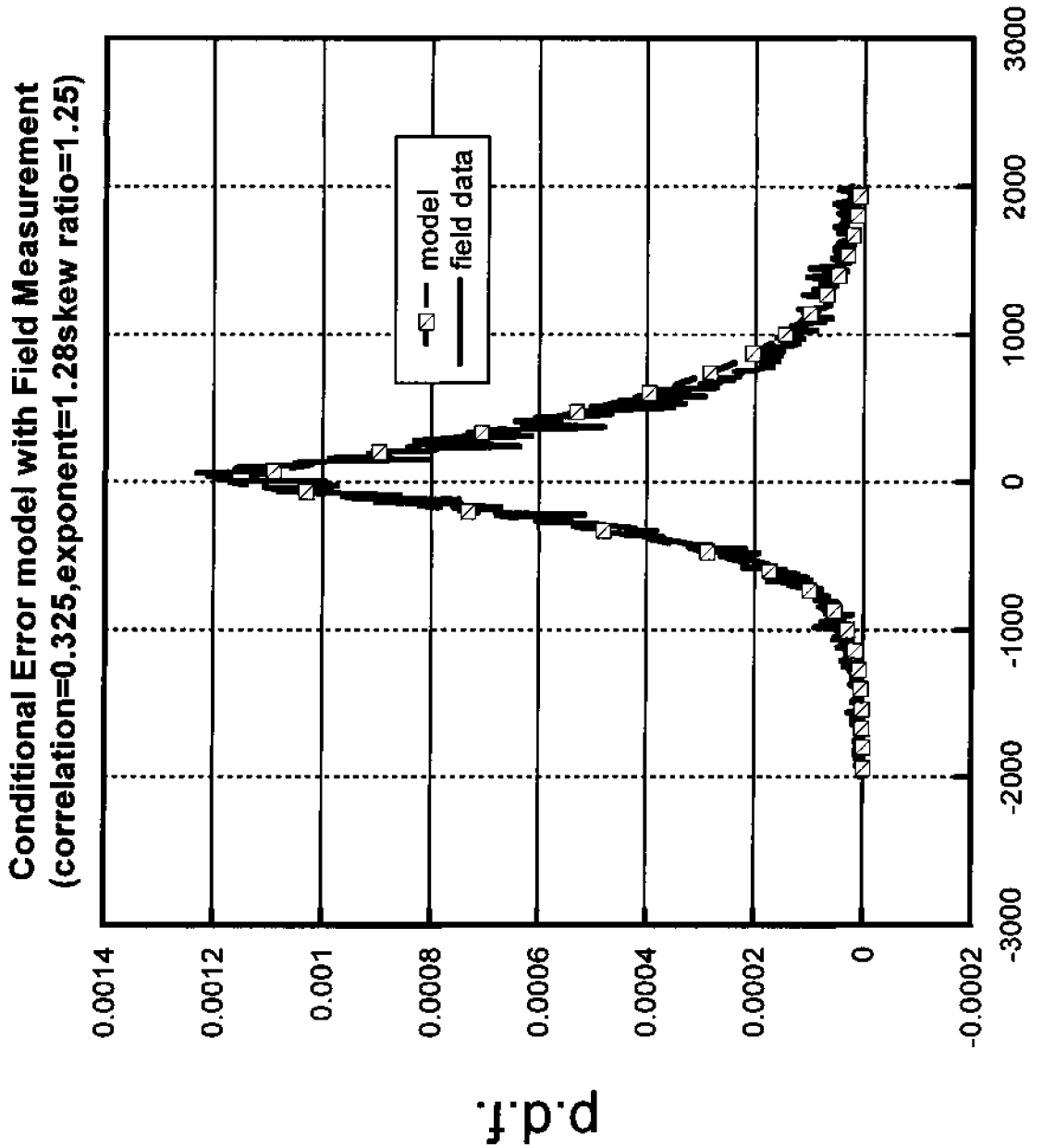
Conditional Error model with Field Measurement
(correlation=0.325,exponent=1.28skew ratio=1.25)
model
field data
p.d.f.
0.0014
0.0012
0.001
0.0008
0.0006
0.0004
0.0002
0
-0.0002
-3000
-2000
-1000
0
1000
2000
3000
TDOA Error (ns)

Figure 13

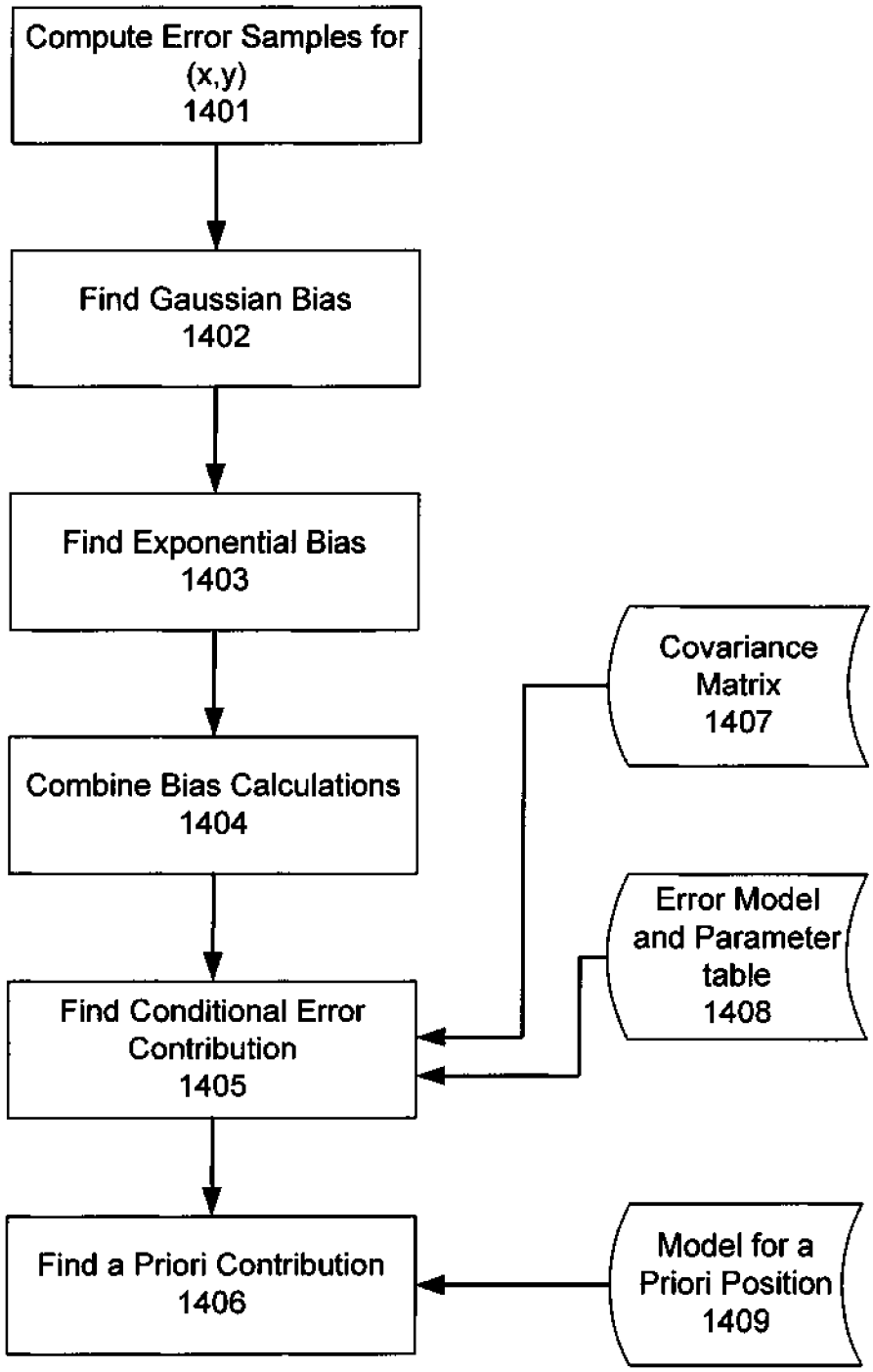
Compute Error Samples for (x,y)
1401
Find Gaussian Bias
1402
Find Exponential Bias
1403
Combine Bias Calculations
1404
Find Conditional Error Contribution
1405
Find a Priori Contribution
1406
Covariance Matrix
1407
Error Model and Parameter table
1408
Model for a Priori Position
1409

Figure 14

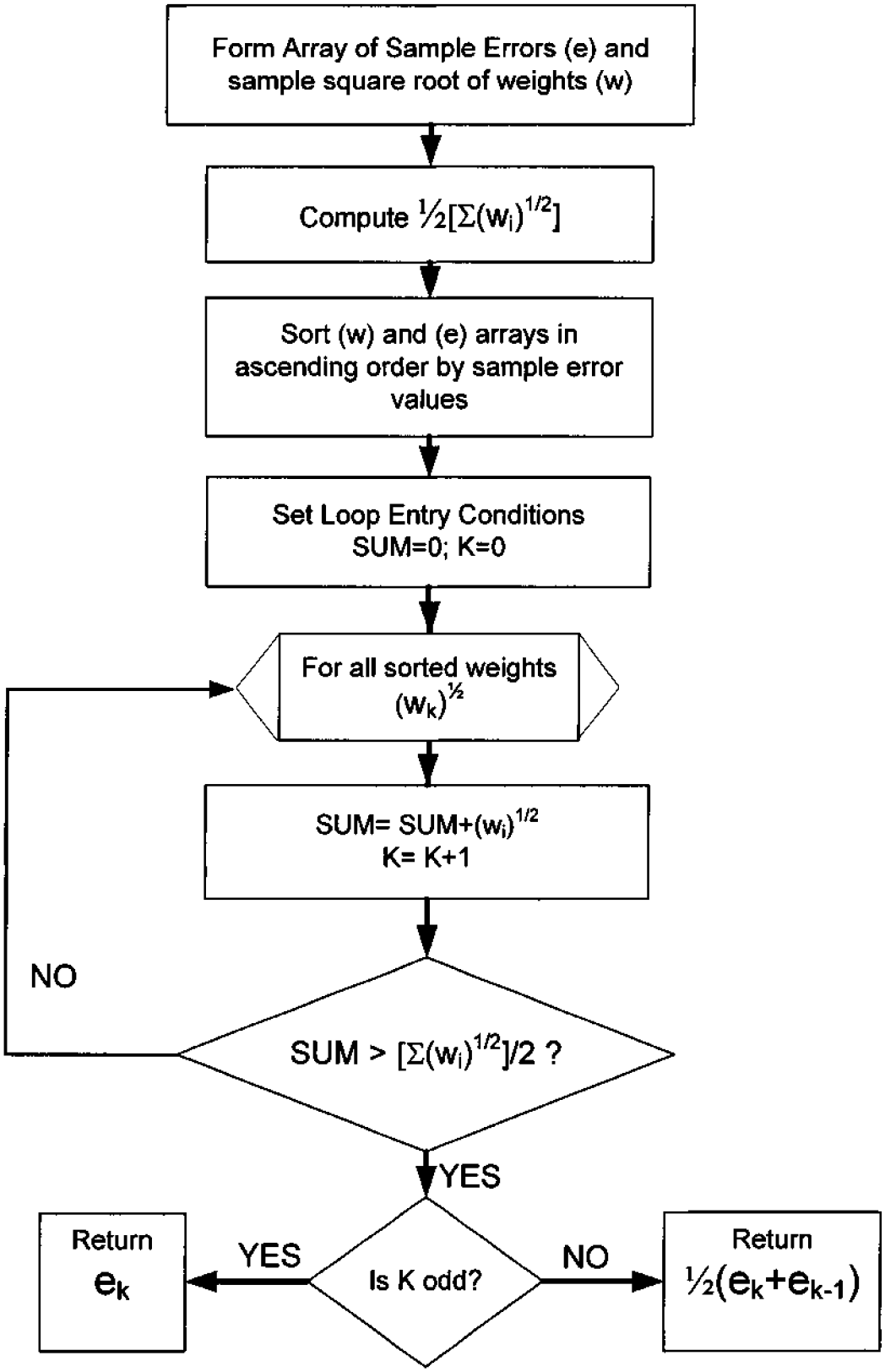
Form Array of Sample Errors (e) and sample square root of weights (w)
Compute ½[Σ(wi)1/2]
Sort (w) and (e) arrays in ascending order by sample error values
Set Loop Entry Conditions SUM=0; K=0
For all sorted weights (wk)½
SUM= SUM+(wi)1/2 K= K+1
NO
SUM > [Σ(wi)1/2]/2 ?
YES
Return ek
YES
Is K odd?
NO
Return ½(ek+ek-1)

Figure 15

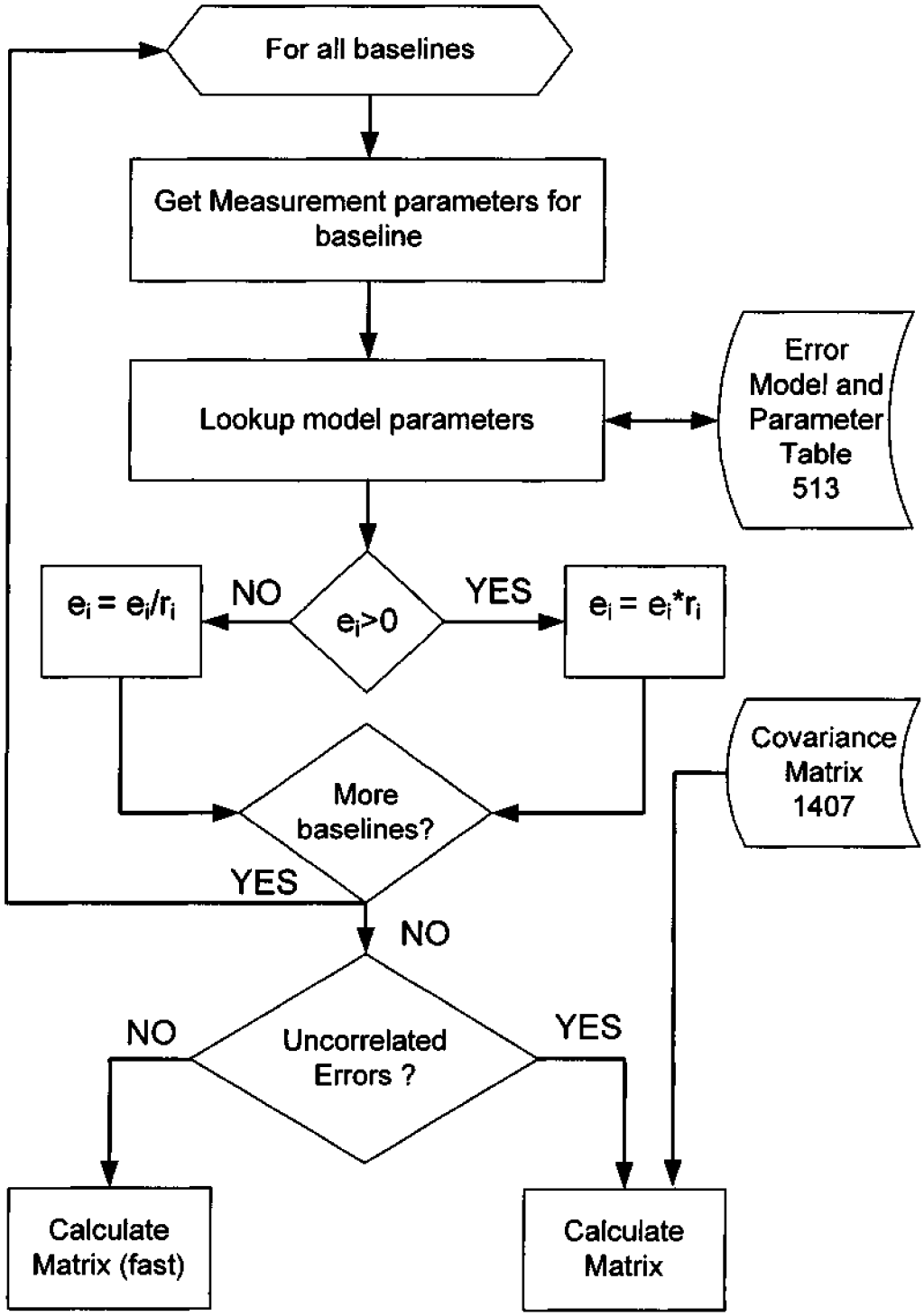
For all baselines
Get Measurement parameters for baseline
Lookup model parameters
Error Model and Parameter Table 513
$e_i = e_i/r_i$
NO
$e_i>0$
YES
$e_i = e_i*r_i$
Covariance Matrix 1407
More baselines?
YES
NO
NO
Uncorrelated Errors ?
YES
Calculate Matrix (fast)
Calculate Matrix

Figure 16

INTERNATIONAL SEARCH REPORT

International application No.
PCT/US2009/067886

A. CLASSIFICATION OF SUBJECT MATTER
IPC(8) - H04B 1/10 (2010.01)
USPC - 455/404.2
According to International Patent Classification (IPC) or to both national classification and IPC

B. FIELDS SEARCHED

Minimum documentation searched (classification system followed by classification symbols)
IPC(8) - H04B 1/10; H04W 24/00 (2010.01)
USPC - 375/349; 455/404.2, 456.1; 701/207

Documentation searched other than minimum documentation to the extent that such documents are included in the fields searched

Electronic data base consulted during the international search (name of data base and, where practicable, search terms used)
MicroPatent, Google Patents, IEEE Xplore, Google Scholar

C. DOCUMENTS CONSIDERED TO BE RELEVANT

Category*	Citation of document, with indication, where appropriate, of the relevant passages	Relevant to claim No.
A	US 2005/0267677 A1 (POYKKO et al) 01 December 2005 (01.12.2005) entire document	1-7
A	US 2005/0281363 A1 (QI et al) 22 December 2005 (22.12.2005) entire document	1-7
A	US 2005/0192024 A1 (SHEYNBLAT) 01 September 2005 (01.09.2005) entire document	1-7
A	US 2004/0002347 A1 (HOCTOR et al) 01 January 2004 (01.01.2004) entire document	1-7
A	US 2007/0247368 A1 (WU) 25 October 2007 (25.10.2007) entire document	1-7
A	US 4,688,187 A (McWHIRTER) 18 August 1987 (18.08.1897) entire document	1-7

☐ Further documents are listed in the continuation of Box C. ☐

* Special categories of cited documents:
"A" document defining the general state of the art which is not considered to be of particular relevance
"E" earlier application or patent but published on or after the international filing date
"L" document which may throw doubts on priority claim(s) or which is cited to establish the publication date of another citation or other special reason (as specified)
"O" document referring to an oral disclosure, use, exhibition or other means
"P" document published prior to the international filing date but later than the priority date claimed
"T" later document published after the international filing date or priority date and not in conflict with the application but cited to understand the principle or theory underlying the invention
"X" document of particular relevance; the claimed invention cannot be considered novel or cannot be considered to involve an inventive step when the document is taken alone
"Y" document of particular relevance; the claimed invention cannot be considered to involve an inventive step when the document is combined with one or more other such documents, such combination being obvious to a person skilled in the art
"&" document member of the same patent family

Date of the actual completion of the international search	Date of mailing of the international search report
04 February 2010	03 MAR 2010
Name and mailing address of the ISA/US Mail Stop PCT, Attn: ISA/US, Commissioner for Patents P.O. Box 1450, Alexandria, Virginia 22313-1450 Facsimile No. 571-273-3201	Authorized officer: Blaine R. Copenheaver PCT Helpdesk: 571-272-4300 PCT OSP: 571-272-7774